fire

Appendix A

1. Valley wind types

Fire behavior is the result of the interaction among topography, fuel and weathers, such as temperature, relative humidity, drought factor, wind magnitude and direction [1]. In particular, wind plays significant roles in fire propagation in rugged terrain and shows various dynamic forms that strongly interact with topography [1–6]. There are four dynamiapnc wind forms: (A) diurnal wind, (B) pressure driven channeling, (C) downward transport of momentum and (D) forced channeling.

The first form of dynamic wind is thermal driven winds. Especially, the wind cycle within a day is called diurnal wind. This type of wind often occurs within valleys. There are four diurnal winds: (A-1) along-slope wind, (A-2) along-valley wind system, (A-3) cross-valley wind system and (A-4) mountain-plain wind system. In along slope system (A-1), the wind blows up the sidewall around dawn and down the wall around dusk. In along valley system (A-2), up along the valley axis during daytime and down along the axis during the night. In addition, the wind also blows from sidewall to sidewall if there is a thermal gap caused by insolation between walls and this type of wind is often called cross-valley system (A-3). The diurnal wind is also observed in a slightly larger scale than valleys. This larger scale wind is called mountain-plain wind system (A-4). The wind blows to a mountain from the same altitude above the plain during daytime and does opposite direction during night. The second wind is (B) pressure driven channeling. A large pressure gradient in synoptic atmosphere generates this channeling. In pressure driven channeling, the wind always blows from high pressure end to low pressure end in the valley while the geostrophic wind aloft proceeds along the isobars, which are the line of constant pressure, regardless of the wind direction in the pressure-driven channeling underneath [2–4]. The below illustrates the direction of the geostrophic winds aloft and the direction of winds by the pressure-driven channeling in the valley.

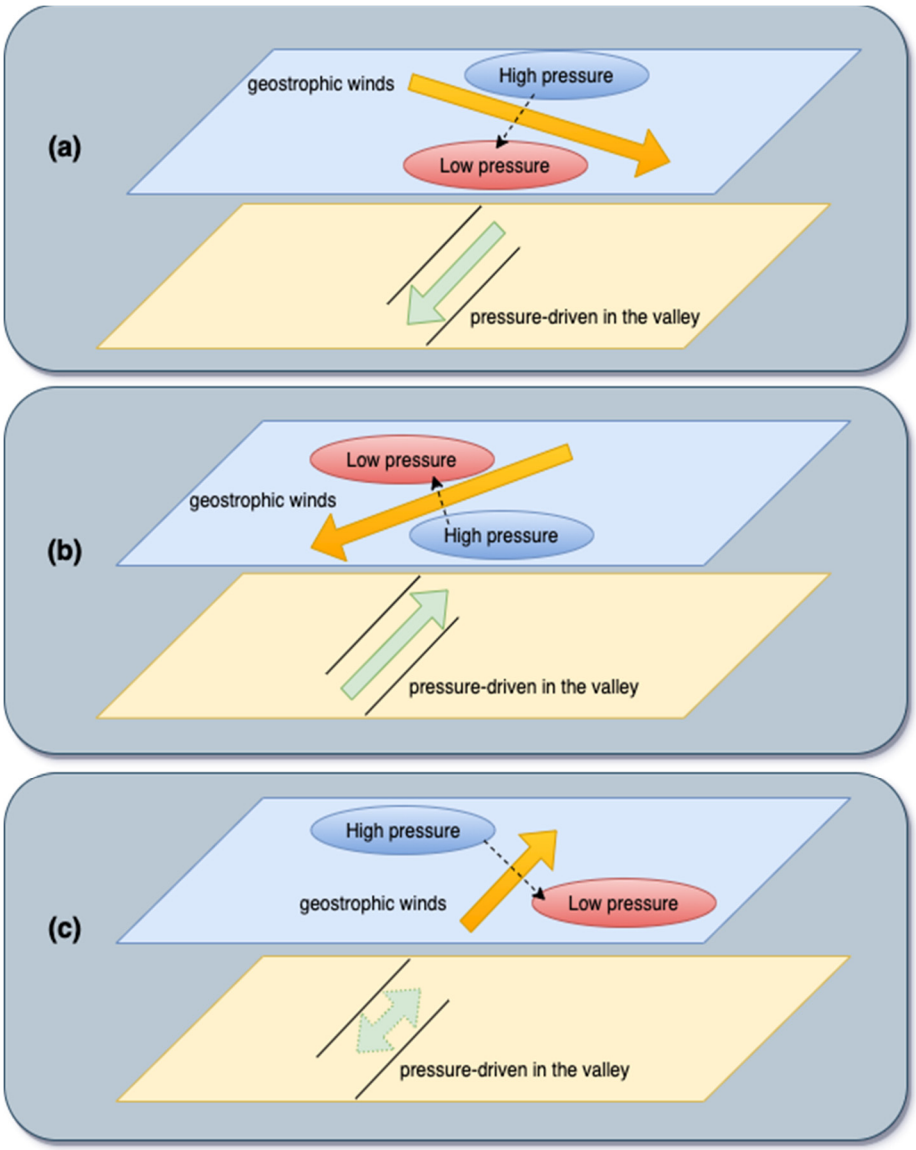

Figure 1: Pressure-driven channeling and geostrophic winds adapted from [2]. While geostrophic wind blows left in the South Hemisphere (right in the North Hemisphere) against the normal lines, which are illustrated with dotted arrows, from high to low atmospheric pressure, the wind in the pressure-driven channeling blows from high to low pressure in the valley in (a) and (b) in the South Hemisphere. Note that pressure-driven wind is ignorable when atmospheric contour lines run parallel to the valley axis seen in (c).

Geostrophic wind blows left in the South Hemisphere (right in the North Hemisphere) against the normal lines, which are represented by dotted arrows, from high to low atmospheric pressure due to the Coriolis Force (CF) according to Bays-Ballot rules while the wind in the pressure driven channeling blows from high to low pressure as mentioned above. The third relevant wind form is (C) downward transport of momentum. The momentum drags the airflow down into the valley when atmosphere is turbulent caused by mixture of synoptic and local atmosphere. The last wind form is (D) forced channel wind in which wind is forced to deflect so that the modified direction aligns with the axis of the valley under the circumstances that friction of the sidewall is much greater than that in the valley axis [4]. For instance, the forced channeling ends up with blowing along the valley when the airflow aloft is taken down into the valley.

Figure 2: In the forced channeling, the synoptic wind is dragged and deflect along the valley axis cited in [2]

Downward transport of momentum is required by forced channeling when the winds blowing aloft parallel to pressure contours are derived from the main stream and diverted into the forced channeling [2]. The direction of the flow in forced channeling could change even 180 ° under specific circumstances [4]. This channel most often occurs during daytime because the status of atmosphere is either neutral or unstable, and the wind speed rapidly increases in this period [2,4]. Interestingly, the forced channel is often observed with foehn windstorm [2]. If this micro- or topo-climate is intercepted by or mixed with the winds aloft, the forced channeling would show the rapid change of fire direction [2–4].

2. Methods and Materials

2.1. Simulation of fire propagation by Prototype 2

Fire propagation is simulated by Prototype 2 with various configurations, such as different downslope distance calculation, rate of fire spreading and geometries of prediction grids against various fire isochrones as observed data. Architecture of Prototype 2 and Experiment results are addressed in the following sub-sections.

2.1.1. System Architecture of Prototype 2

Prototype 2 has been developed not only for Riveaux Road fire but also for other regions in Australia to simulate a fire propagation. The general architecture of the Prototype 2 is shown below.

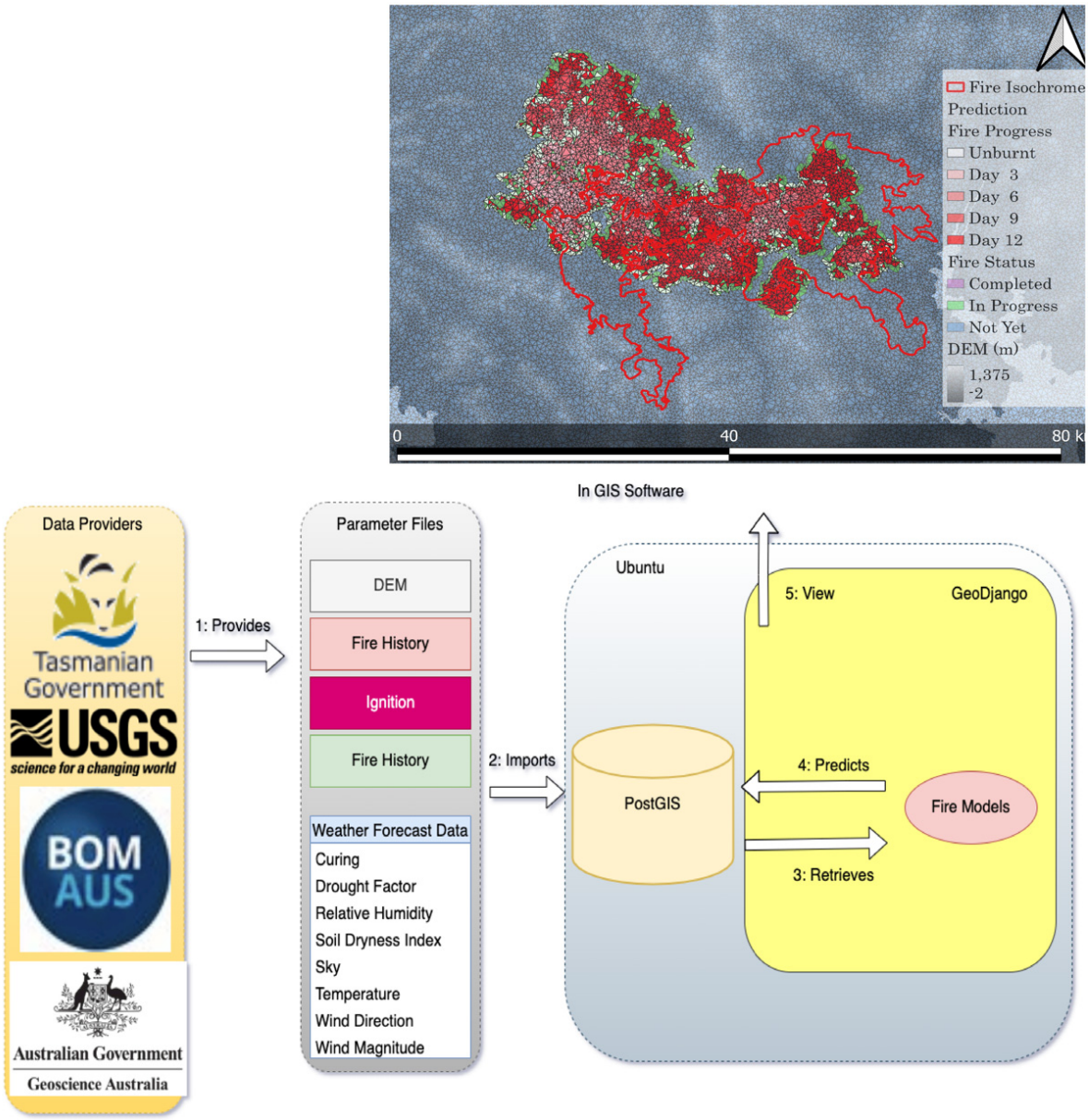

Figure 3: System architecture of Prototype 2.

The operating system in which the Prototype 2 runs is Ubuntu 20.04, which is a Linux based system [7]. This prototype was implemented by using GeoDjango 2.0, which is a python-framework, Django, with various geographical functions [8]. The database management system is PostGIS 3.1, which is the extension of PostgreSQL, and contains geographical functions [9]. The various data, such as digital elevation model (DEM), vegetation polygons, surface weather, observed fire and fire prediction grids, are stored in the PostGIS database as spatial tables and the prototype retrieves these data by communicating with the PostGIS. Fire prediction data are simultaneously updated in the database as the simulation is run, with results ultimately viewable within GIS software, such as QGIS.

2.1.2. Experiment round

An experiment round consists of

1. Fire isochrones as the observed data
2. Katabatic slope distance
3. Elapse coefficient and
4. Fire prediction geometries: Delaunay, Diamond, Hexagon, Square and Voronoi

Firstly, each fire is simulated for a fire isochrone by using the same ignitions so that the result can be compared with fire isochrone as ground truth. Secondly, two types of katabatic slope distance, such as plan/projected (2D) and linear/ground (3D), are employed in turn. Thirdly, the total elapse of fire simulation is taken into account for other fire simulations to adjust the elapse to approach to the ground truth so that a fire event in each grid can be occurred in the close timing to the ground truth. These three conditions are combined differently in experiment rounds. Fourthly, five geometries are employed in each round as random sampling.

An example above combinations is as following. The plan/projected katabatic slope distance is selected, and no elapse coefficient is configured in round 20. All geometries are ingested for simulation against fire isochrone #1 in this round. Round 22 carries over the round 20 with the elapse adjustment.

Each simulation finishes when a total burnt area reaches that of ground truth, the fire isochrone. The experiment result whose burning duration is the closest to the ground truth, is selected in each geometry and katabatic slope distance. See the Appendix 2 [10].

2.1.3. Two types of ROS coefficient

Rate of fire spreading (ROS) is a common output of core fire models, such as CSIRO Grassland fire spread model. There are two coefficients for the ROS in Prototype 2. One is a slope distance coefficient, and another is an elapse adjustment. Further, there are three types of slope distance coefficient to the ROS. The first is the distance for uphill and used for all simulations. The second and third are for the downslope distance. These downslope distances are plan/projected (2D) and linear/ground (3D). The plan/projected distance is 2-dimensional cartesian distance and designed for large scale while the linear/ground distance is 3-dimensional distance and for small scale [11,12] as seen below.

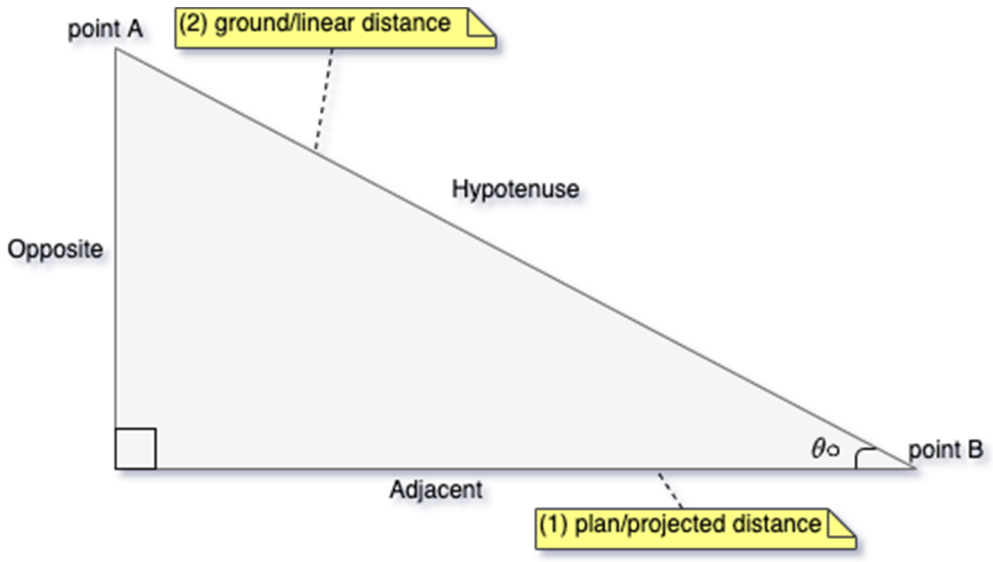

Figure 4: Katabatic slope distances: plan/project and linear/ground distance

Either katabatic slope distance is selected by configuration. The further details of slope distance are addressed in Appendix 2 [10].

Another coefficient is elapse adjustment. This coefficient is necessary because magnitude of the total elapse varies among fire geometries. That is, frequency to calculate elapse in simulation grid is associated to the number of its immediate neighbor grids. For instance, elapse in Delaunay tends to be the shortest because it has approximately 12.5 neighbors, which is more than that of other geometries. Therefore, the elapse is adjusted by multiplying the elapse coefficient calculated from the previous set of experiment, so-called round.

2.2. Data structure and process

Since Prototype 2 consists of several fire models, various geodata are ingested. There are two types of geospatial data: vector and raster. Both types are stored, retrieved, and updated in the database by Prototype 2 to simulate fire propagation. The prefix of the table name is riveaux_ for the Riveaux Road fire as seen below.

Table 1: Database tables for the Riveaux Road Fire, which starts by either riveaux_

Database table name	Type	Description
riveaux_version	Vector	Version record. See external appendix [10].
riveaux_vegetation	Vector	Vegetation data
riveaux_history	Vector	Fire history
riveaux_ignition	Vector	Ignition record
riveaux_ignitionincident	Vector	Ignition incident record
riveaux_lightning	Vector	Lighting hit record
riveaux_geology	Vector	Geology record
riveaux_delaunay	Vector	Delaunay shape prediction
riveaux_diamond	Vector	Diamond shape prediction
riveaux_hexagon	Vector	Hexagon shape prediction
riveaux_square	Vector	Square shape prediction
riveaux_voronoi	Vector	Voronoi shape prediction
riveaux_delaunaycentroid	Vector	Centroid for Delaunay prediction
riveaux_diamondcentroid	Vector	Centroid for Diamond prediction
riveaux_hexagoncentroid	Vector	Centroid for Hexagon prediction
riveaux_squarecentroid	Vector	Centroid for Square prediction
riveaux_voronoicentroid	Vector	Centroid for Voronoi prediction
riveaux_ras	Raster	Raster table for DEM, curing and climate data
riveaux_band	Standard	Raster band table for raster
riveaux_category	Standard	Community category for vegetation metadata
riveaux_community	Standard	Community for vegetation metadata
riveaux_firemodel	Standard	Fire model for vegetation metadata
riveaux_flammability	Standard	Flammability for vegetation metadata
riveaux_sensitivity	Standard	Sensitivity for vegetation metadata
riveaux_vegmeta	Standard	Bridging table with vegetation, flammability, sensitivity, community, and fire models

2.2.1. Vector spatial data

- Vegetation data

The Listmap provides various spatial data. Vegetation distribution is vector data and retrieved from Listmap [13]. Two versions of vegetation geodata are employed. One is TASVEG3 and another is TASVEG4. TASVEG4 was released during this research with some error corrections such as removal of overlap polygons. Fortunately, both versions contain the vegetation data in Riveaux Road Fire because the data were compiled before the date of the wildfire. That is, the completion data is 18/11/2013 in both TASVEG3 and TASVEG4. With regard to coordinate system, it is not necessary to reproject because both vegetation data have already been GDA94 zone 55 (SRID: 28355). However, an extra process is necessary for both versions. In TASVEG 3, the vegetation data are merged by QGIS because these are separately distributed. Then they are imported into the database as seen below.

Table 2: Processes of TASVEG3 in Tasmania

#	Step name	Description
1	Merge	TASVEG3 datasets are merged.

2	Import to database	TASVEG3 is imported into the database.

In terms of TASVEG4, it is necessary to diminish its extent because the original coverage is whole TASMANIA. The process of TASVEG4 to fit this study area is as seen below.

Table 3: Processes of TASVEG4 in Tasmania

#	Step name	Description
1	Creation of extent polygon	Extent polygon which covers the study area and its surroundings only, is generated in QGIS.
2	Import to database	TASVEG4 and the extent polygon are imported into the database.
3	Clip	TASVEG4 is clipped in QGIS.
4	Export	For analysis purpose, clipped data are exported so that it can be viewed in QGIS.
5	Import to database	TASVEG4 is imported into the database.

There is an issue in the clipping function in QGIS because this function produced missing data. In order to circumvent this issue, the whole data are imported in PostGIS database with an extent polygon and only data covering study area is clipped by the extent polygon using PostGIS function. The clipped data are exported so as to analyze it in QGIS and imported back to PostGIS for simulation. The main features of the TASVEG3 and TASVEG4 are seen in below.

Table 4: Vegetation table structure

Column	Description
FOREST_STR	forest string
SOURCE_DAT	yyyy-MM-dd
LIST_GUID	GUID
VEGCODE_D	vegetation code detail
VEG_GROUP	vegetation group

Note that a vegetation class is implemented by inheriting the abstract vegetation class, which is a common class in the system, so that regionally specific features are only taken into account in this study area and do not have an impact on other study areas (See external appendix, Fire Simulator) [10].

There are some supportive tables for vegetation in this study area. The vegetation meta table (riveaux_vegmeta) is a mapping table for additional information such as fire models, flammability, sensitivity, and vegetation community as seen below.

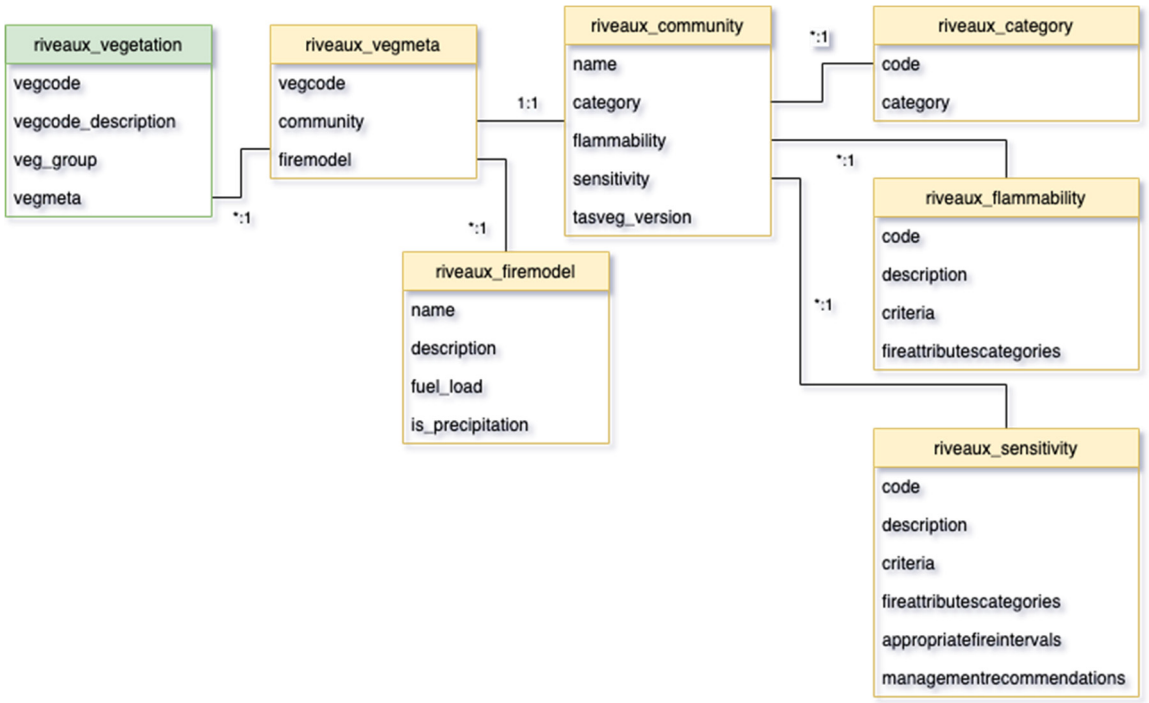

Figure 5: UML class diagram for TASVEG4 and vegetation community

A fire model table (*riveaux_firemodel*) comprises of fuel load and precipitation, which are ingested in the fire model in addition to the name of fire model. This table allows the system to select an appropriate fire model by the vegetation on the location. A vegetation community table (*riveaux_community*) maps flammability (*riveaux_flammability*) and sensitivity (*riveaux_sensitivity*) of vegetation [14]. These tables are reused from the previous prototype with an additional record for TASVEG4. This additional record is "Improved pasture with native tree canopy (FAC)", which belongs to Modified land vegetation group and assigned to high flammability, low sensitivity and FireShrublandBelowWoodland model by considering the canopy coverage more than 5 % in this prototype [13]. Note that the fire model table comes into play after round 16.

- Geology

  A geology table represents mineral distribution. This table is necessary to calculate a rate of fire spreading (ROS) in buttongrass moorland area. Structure of geological data are described in the external appendix [10].

- Fire History

  Although the fire propagates from 15th January till 24th March in 2019, the simulations are executed till 1st February in 2019 at most because of the limitation of obtainable data. However, these periods cover the fire propagation in the Riveaux Road Fire, which is the focus in this study area as seen below.

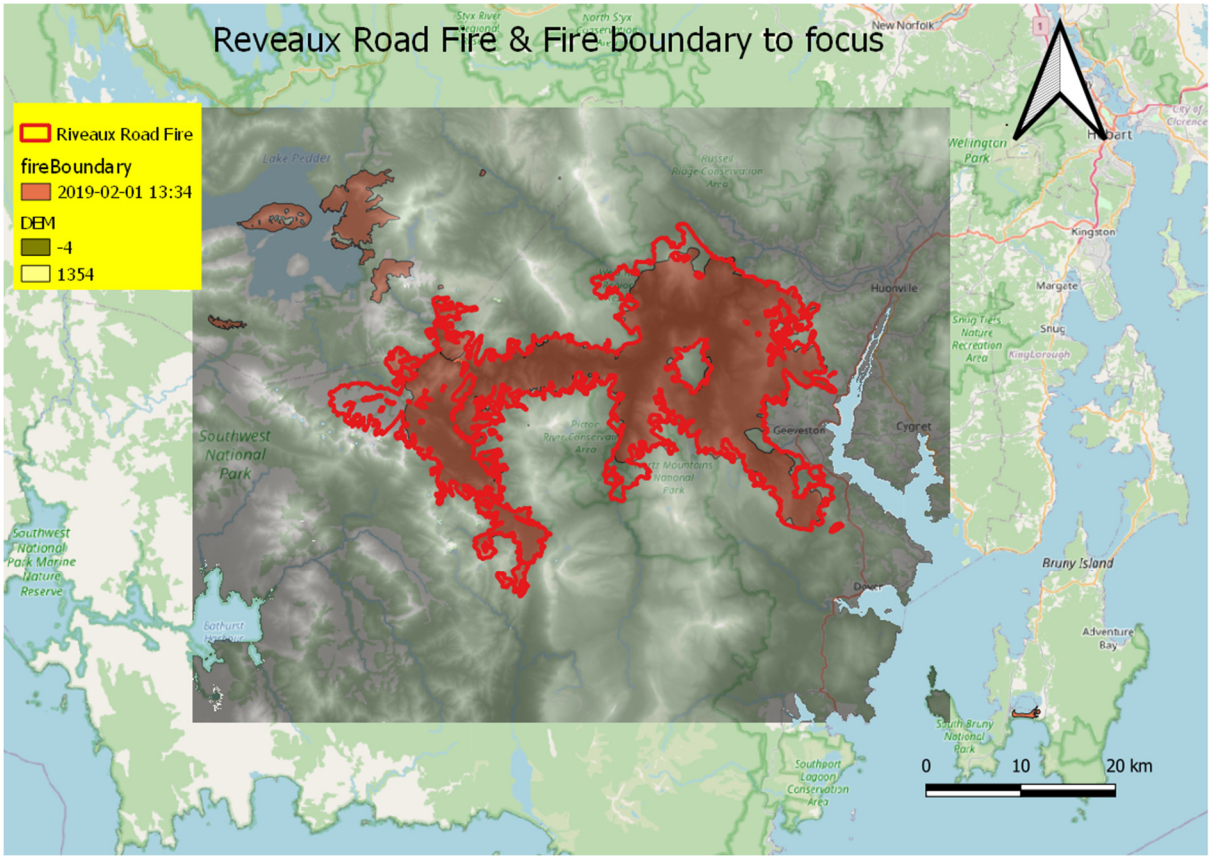

Figure 6: Total fire period and focused period in Riveaux Road Fire

Note that the smaller isochrones were incorporated later on for analysis of fire behaviours in individual isochrones.

Similar to the vegetation, the fire history table is a vector file and retrieved from Listmap [13]. Then it is imported into the database. The structure of the fire history is seen below.

Table 5: Structure of a fire history in Tasmania

Column	Description
INCD_NO	forest string
INCD_START	yyyy-MM-dd
INCD_END	yyyy-MM-dd
FIRE_NAME	Fire name
FIRE_TYPE	Fire type
IGN_DATE	Ignition date
IGN_CAUSE1	Reason of ignition 1
IGN_CAUSE2	Reason of ignition 2
SHAPE_AREA	area
SHAPE_LEN	length of polygon

Similar to the vegetation class, the fire history class is implemented by inheriting the abstract class (See external appendix) [10].

- Fire Isochrones

Three fire isochrones are employed as observed data for Riveaux Road Fire. The below table shows durations, burnt areas and sizes of prediction polygons for each fire isochrone.

Table 6: Fire isochrones with duration of fire, area, elevation of highest and lowest location as well as altitudinal gap. The fire isochrone #1 shows the least gap while #3 shows the most gap.

#	Start	End	Areas (km^2)	Highest (m)	Lowest (m)	Elevation gap (m)
1	18th January	22nd January	9.94	390	55	335
2	16th January	24th January	6.17	738	167	571
3	20th January	24th January	9.77	765	146	619

The below figure shows the fire isochrones.

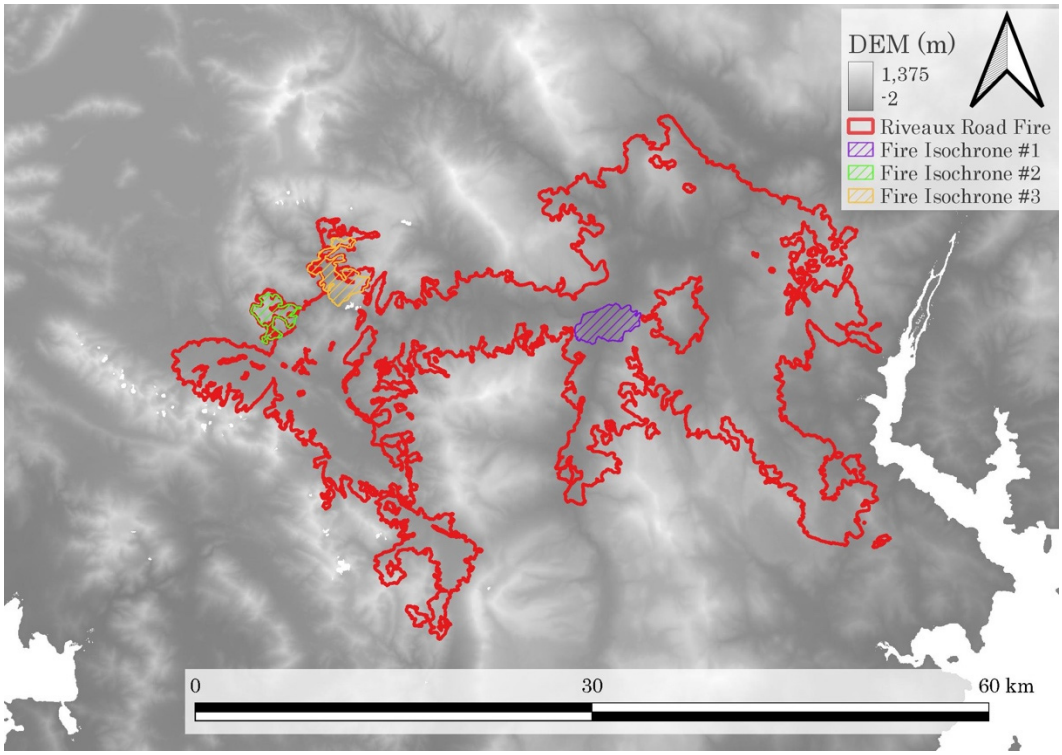

Figure 7: There are three fire isochrones: (#1) the east in purple occurred from 18th in local time, (#2) the west isochrone in light-green occurred from 16th, (#3) the north isochrone in orange started on 20th.

Table 7: Fire isochrones with areas and elevations.

#	Start	End	Areas (km^2)	Elevation Gap (lowest: highest) in meters
1	18th January	22nd January	9.94	335 (55:390)
2	16th January	24th January	6.17	571 (167:738)
3	20th January	24th January	9.77	619 (146:765)

In accordance with the elevation gap, fire isochrones are listed from the least to the most rugged.

- Ignition Incident
  Ignition incident table is optionally ingested for identifying incident location and time as seen below.

Table 8: Ignition incident table

Column	Description
ENABLED [1]	This field contained whether or not it is verified. Only enabled fields are selected by the system.
OBJECT_ID	Unique id from the provider
INCIDENT_ID	Incident id and name are paired.
INCIDENT_NAME	Incident id and name are paired.
TFS_SOURCE [2]	Timestamp in local time.
STATUS	Either in [Going, Stop, Being Controlled, Patrol, Contained, or Under Control]
AGENCY	Either in [ATFS / PARKS, ATFS, PWS, ATFS, PWS, STT, ATFS, STT, Forestry, FORESTRY, Parks & Wildlife, Parks & Wildlife Service, Parks & Wildlife Service, Parks and Wildlife, Parks And Wildlife, PARKS AND WILDLIFE, Parks and Wildlife Service, Parks and Wildlife Services, Parks and Wildlife Service, Ta, PARKS TFS STT, PARKS, TFS, STT, Sustainable Timber Tasmania, Tasmania Fire Service, Tasmania Fire Service and Park, TFS and Parks and Wildlife Ser]
SIZE	Nullable
FIRETYPE	Either in [ASSIST AMBULANCE, Chimney fire, COMMUNITY SERVICE, ELECTRICAL PROBLEM, FALSE CALLOUT, FIRE INCIDENT, FUEL REDUCTION BURN, MARINE INCIDENT, MVA, POWER POLE FIRE, RESCUE, ROC, RUBBISH FIRE, SHIP OR BOAT FIRE, STRUCTURE FIRE, VEGETATION FIRE, VEHICLE FIRE]

[1] Enabled field represents whether or not this record is verified and only enable fields are employed as ignition points.

[2] TFS_SOURCE filed is the string type and indicates the local date and time. Therefore, it is converted to UTC for consistency in Prototype 2.

- Lightning Hits

Lightning hit dataset is alternative to the ignition incident and is a vector data obtained by GPATS with Time Difference of Arrival (TDOA) method. Because a lightning strike can be detected as a transmission of a radio signal source, location of the lighting hit can be calculated by difference between receivers if there are more than three receivers. The accuracy is less than 250 m and the detection efficiency is more than 95 % and 80 % with cloud-ground and cloud-cloud discharge respectively [15]. In prototype 2, this dataset is imported into the database. Structure of the table is seen below.

Table 9: Structure of lightning hit table

Column	Description
LAT	latitude
LON	Longitude
DATE	yyyy-MM-dd (UTC)
TIME	HH:mm:ss (UTC
AMPS	Amperage (kilo amperes)

- Prediction of fire propagation

There are two geometry sizes: large size is equivalent to a square grid with 500 m side and small size is equivalent to a square grid with 250 m side. These polygons are selected depending upon the areas of observed data, which is a fire isochrone. Data structure of prediction polygon follows the standard format in Prototype 2. See external appendix [10].

2.2.2. Raster spatial data

- Data for Prototype 2

  There are several types: relative soil moisture (upper layer), curing, resampled wind data field, and other climate data as well as digital elevation model (DEM). The relative soil moisture (upper layer) was provided by collaborated project among CSIRO Marine and Atmospheric Research (CMAR), the Bureau of Metrology (BoM), the Bureau of Rural Sciences (BRS) [16]; the wind data are resampled and downscaled by WindNinja; other climate data are mainly from BoM and DEM is from Geoscience Australia. In terms of the wind data resampled by WindNinja, the diurnal wind option is on for the analysis of valley winds. The details are described in external appendix [10].
- Wind Fields

  Wind fields are helpful to identify anomalous wind behavior in rugged terrain. The wind field in BARRA consists of u and v component, which are converted into wind speed and wind direction. BARRA data has an advantage over WindNinja while its resolution is coarser than that of WindNinja. The wind fields can take into account various dynamic winds because BARRA data are assimilation data, which is corrected with observed data. There are two ways of inputting wind data: domain average initialization (WN-DAI) and gridded initialization (WN-GI). The former ingests one point wind data per episode while the latter accept grid-base wind field [17].

3. Results

3.1. Cross section

Amount of conducive structures were measured in each isochrone by cross-section diagram. This diagram shows the vertical atmospheric profile with horizontal coordinate, either latitude or longitude. Target locations were determined either along or perpendicular to either ridges or valleys around ignition points in advance. Then the wind data for the cross-section were interpolated from BARRA-TA datasets and the result of the wind were either tangential or normal to the axis. These plots were viewed as two-dimensional, altitudinal and either latitudinal or longitudinal level. The below figure shows the example of cross-section of relative humidity. There is a contour map for geopotential height of the 950 hPa pressure level at top left in the figure.

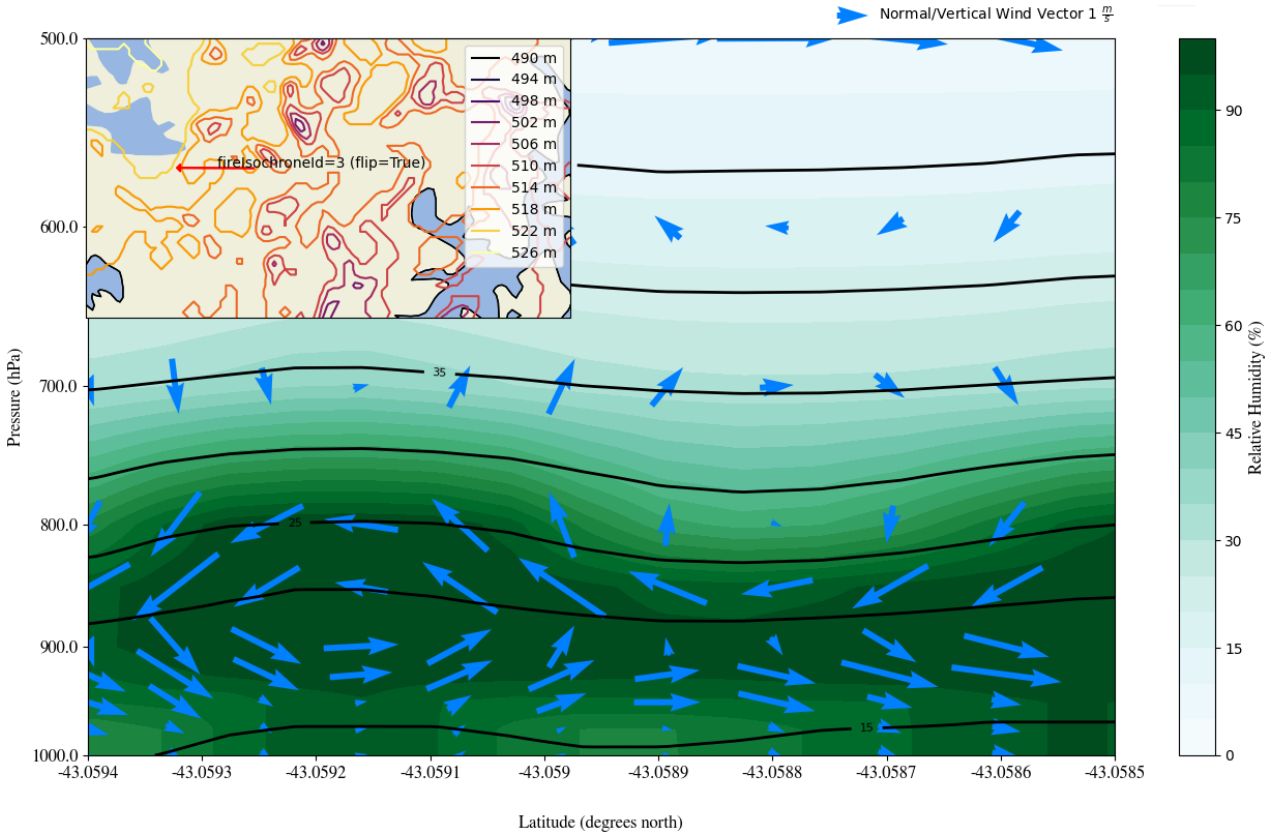

Figure 8: Cross section with relative humidity (%) and wind vector with its magnitude (ms^{-1}).

The number of the plots which contained significant wind change were then counted. Significant wind is here defined as either directional or magnitude change between 900 hPa and 1000 hPa because there are three fire isochrones in these pressure levels. Duration was calculated from the first ignition and the recorded datetime of each observed data. Therefore, the total number of plots varies between isochrones. The below tables show the ratio of weather containing dynamic wind changes.

Table 10: The percentage of cross-section plots containing drastic wind changes for fire isochrone #1 (1499) is 6.51 % in total.

interpolation	Horizontal coordinate	Along/perpendicular	# Significant wind change	Total	%
Tangential	Latitude	Along	0	98	0.00
Tangential	Latitude	Perpendicular	35	98	35.71
Tangential	Longitude	Along	0	98	0.00
Tangential	Longitude	Perpendicular	15	98	15.31
Normal	Latitude	Along	0	98	0.00
Normal	Latitude	Perpendicular	0	98	0.00
Normal	Longitude	Along	1	98	1.02

Normal	Longitude	Perpendicular	0	98	0.00
Total			51	784	**6.51**

Table 11: The percentage of cross-section plots containing drastic wind changes for fire isochrone #2 (1547) is 11.56 % in total.

interpolation	Horizontal coordinate	Along/perpendicular	# Significant wind change	Total	%
Tangential	Latitude	Along	37	200	16.50
Tangential	Latitude	Perpendicular	7	200	3.50
Tangential	Longitude	Along	38	200	19.00
Tangential	Longitude	Perpendicular	2	200	1.00
Normal	Latitude	Along	8	200	4.00
Normal	Latitude	Perpendicular	42	200	21.00
Normal	Longitude	Along	8	200	4.00
Normal	Longitude	Perpendicular	47	200	23.50
Total			185	1,600	**11.56**

Table 12: The percentage of cross-section plots containing drastic wind changes for fire isochrone #3 (1548) is 40.15 % in total.

interpolation	Horizontal coordinate	Along/perpendicular	# Significant wind change	Total	%
Tangential	Latitude	Along	68	113	60.18
Tangential	Latitude	Perpendicular	11	113	9.73
Tangential	Longitude	Along	84	113	74.34
Tangential	Longitude	Perpendicular	10	113	8.85
Normal	Latitude	Along	8	113	7.08
Normal	Latitude	Perpendicular	86	113	76.11
Normal	Longitude	Along	13	113	11.50
Normal	Longitude	Perpendicular	83	113	73.45
Total			363	904	**40.15**

3.2. Simulation of fire propagation by Prototype 2 with BARRA-TA

Three rounds of experiment for fire isochrone #1, #2 and #3 were simulated by ingesting BARRA-TA wind filed. Each area of these area is less than $10km^2$. The motivation of the simulation with BARRA-TA is the interaction with upper air because this dataset is an assimilated with observed data. Whereas, disadvantage is coarseness, approximately $1.5km^2$ while the resample wind by WindNinja takes into account air flow along topographical features in phase, such as diurnal wind, with finer resolution. In other word, vertical interaction is well-considered in BARRA-TA while surface or horizontal interaction is considered by WindNinja. The scores with BARRA-TA show better than the one with the resample wind where there were turbulent air flows aloft.

3.2.1. Fire isochrone #1 (ID1499) from 18th till 22nd January 2019 (local time)

In experiments, small prediction polygons are employed. The results of elapse are shown below.

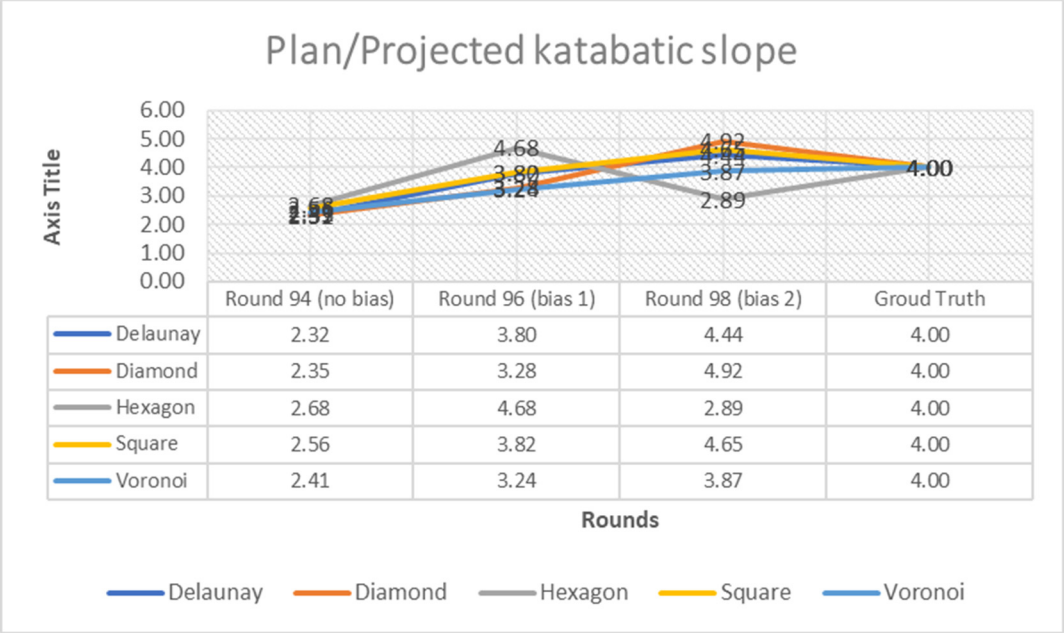

Figure 9: Elapses in the plan/projected katabatic slope (2D) distance for fire isochrone #1.

The closest round in Voronoi is round 98 while the one for other geometries is the round 96.

Table 13: Verification scores with 2D in fire isochrone #1 from five geometries, Delaunay (R96), Diamond (R96), Hexagon (R96), Square (R96) and Voronoi (R98).

Verification method	**Indicator**	**Delaunay**	**Diamond**	**Hexagon**	**Square**	**Voronoi**	**Average score**
Completion Rate [1]		1.00	1.00	1.00	1.00	1.00	1.00
Cohen's Kappa Score	-	0.60	0.62	0.53	0.60	0.66	0.60
	Gap from another slope distance	-0.02	0.25	0.19	0.04	0.18	0.13
Fractions Skill Score (FSS)	-	0.69	0.69	0.60	0.70	0.75	0.68
	Gap from another slope distance	-0.02	0.27	0.20	0.04	0.19	0.14
Confusion Matrix	Useful	0.50	0.50	0.50	0.50	0.50	0.50
	Accuracy	1.00	1.00	1.00	1.00	1.00	1.00
	Gap from another slope distance	-0.00	0.00	0.00	0.00	0.00	0.00
	Misclassification Rate	0.00	0.00	0.00	0.00	0.00	0.00
	Precision	0.77	0.80	0.68	0.75	0.83	0.77
	Gap from another slope distance	-0.03	0.32	0.24	0.05	0.22	0.16
	Specificity	1.00	1.00	1.00	1.00	1.00	1.00
	Prevalence	0.00	0.00	0.00	0.00	0.00	0.00
	True Positive Rate	0.49	0.51	0.43	0.50	0.55	0.49
	False Positive Rate	0.00	0.00	0.00	0.00	0.00	0.00
	Threat score [2]	0.43	0.45	0.36	0.43	0.49	0.43
	Gap from another slope distance	-0.02	0.22	0.15	0.04	0.18	0.12

[1] Completion Rate is the ratio of total burnt area of prediction against observed data. [2] Threat score is originally independent indicator from confusion matrix; however, it is included in confusion matrix in this study because the parameters in confusion matrix are used in this indicator.

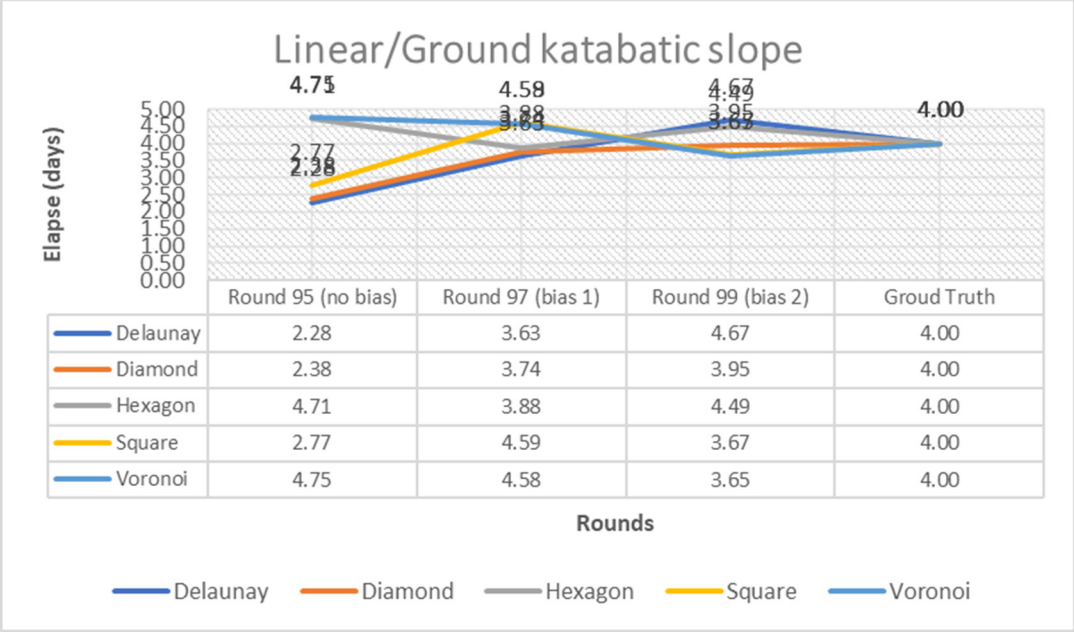

Figure 10: Elapses in the linear/ground katabatic slope (3D) distance for fire isochrone #1.

The closest round in Delaunay and Hexagon is round 97 while the one for other geometries is the round 99.

Table 14: Verification scores with 3D in fire isochrone #1 from five geometries, Delaunay (R97), Diamond (R99), Hexagon (R97), Square (R99) and Voronoi (R99).

Verification method	**Indicator**	**Delaunay**	**Diamond**	**Hexagon**	**Square**	**Voronoi**	**Average score**
Completion Rate [1]		1.00	1.00	1.00	1.00	1.00	1.00
Cohen's Kappa Score	-	0.62	0.37	0.34	0.56	0.48	0.47
	Gap from another slope distance	0.02	-0.25	-0.19	-0.04	-0.18	-0.13
Fractions Skill Score (FSS)	-	0.71	0.42	0.40	0.66	0.56	0.55
	Gap from another slope distance	0.02	-0.27	-0.20	-0.04	-0.19	-0.14
	Useful	0.50	0.50	0.50	0.50	0.50	0.50

Confusion Matrix	Accuracy	1.00	1.00	1.00	1.00	1.00	1.00
	Gap from another slope distance	0.00	-0.00	-0.00	-0.00	-0.00	-0.00
	Misclassification Rate	0.00	0.00	0.00	0.00	0.00	0.00
	Precision	0.80	0.47	0.44	0.70	0.61	0.60
	Gap from another slope distance	0.03	-0.32	-0.24	-0.05	-0.22	-0.16
	Specificity	1.00	1.00	1.00	1.00	1.00	1.00
	Prevalence	0.00	0.00	0.00	0.00	0.00	0.00
	True Positive Rate	0.51	0.30	0.28	0.46	0.39	0.39
	False Positive Rate	0.00	0.00	0.00	0.00	0.00	0.00
	Threat score [2]	0.45	0.22	0.21	0.39	0.31	0.31
	Gap from another slope distance	0.02	-0.22	-0.15	-0.04	-0.18	-0.12

[1] Completion Rate is the ratio of total burnt area of prediction against observed data. [2] Threat score is originally independent indicator from confusion matrix; however, it is included in confusion matrix in this study because the parameters in confusion matrix are used in this indicator.

3.2.2. Fire isochrone #2 (ID1547) from 16th till 24th January 2019 (local time)

In experiments, small prediction polygons are employed. The results of elapse are shown below.

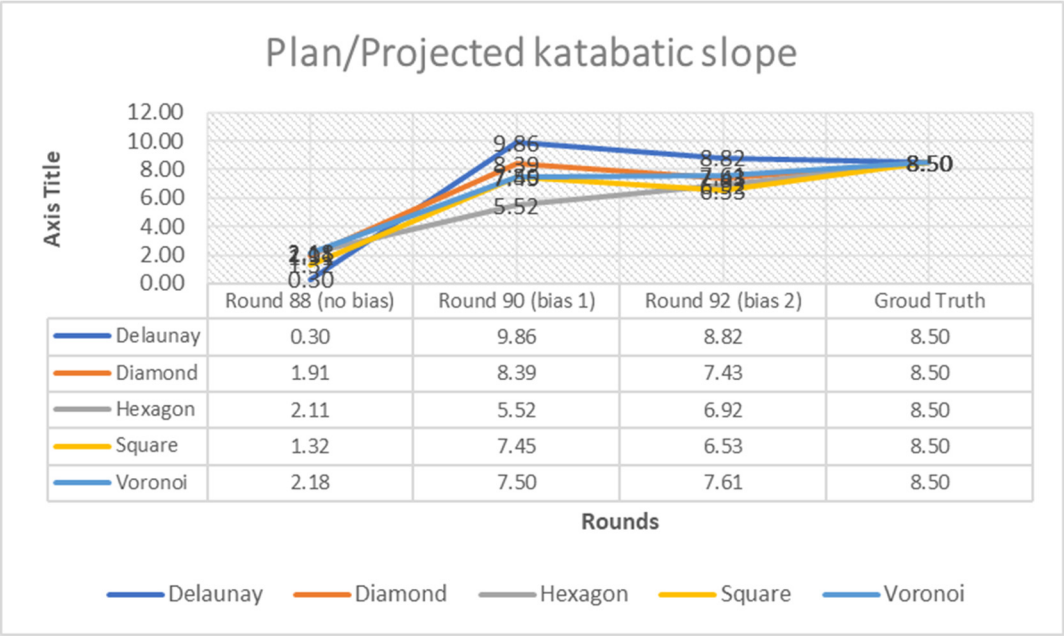

Figure 11: Elapses in the plan/projected katabatic slope (2D) distance for fire isochrone #2.

The closest round in Diamond and Square is round 90 while the one for other geometries is round 92.

Table 15: Verification scores with 2D in fire isochrone #2 from five geometries, Delaunay (R92), Diamond (R90), Hexagon (R92), Square (R90) and Voronoi (R92).

Verification method	Indicator	Delaunay	Diamond	Hexagon	Square	Voronoi	Average score
Completion Rate [1]		1.00	1.00	1.00	1.00	1.00	1.00
Cohen's Kappa Score	-	0.41	0.47	0.60	0.52	0.38	0.48
	Gap from another slope distance	0.00	0.02	0.33	0.14	-0.06	0.09
Fractions Skill Score (FSS)	-	0.51	0.56	0.68	0.65	0.47	0.58
	Gap from another slope distance	0.01	0.04	0.36	0.17	-0.06	0.10
Confusion Matrix	Useful	0.50	0.50	0.50	0.50	0.50	0.50
	Accuracy	1.00	1.00	1.00	1.00	1.00	1.00
	Gap from another slope distance	0.00	0.00	0.00	0.00	-0.00	0.00
	Misclassification Rate	0.00	0.00	0.00	0.00	0.00	0.00
	Precision	0.72	0.77	1.00	0.86	0.65	0.80
	Gap from another slope distance	0.03	0.04	0.56	0.22	-0.09	0.15
	Specificity	1.00	1.00	1.00	1.00	1.00	1.00
	Prevalence	0.00	0.00	0.00	0.00	0.00	0.00
	True Positive Rate	0.29	0.34	0.43	0.38	0.27	0.34
	False Positive Rate	0.00	0.00	0.00	0.00	0.00	0.00
	Threat score [2]	0.26	0.31	0.43	0.36	0.24	0.31
	Gap from another slope distance	0.00	0.02	0.27	0.11	-0.05	0.06

[1] Completion Rate is the ratio of total burnt area of prediction against observed data. [2] Threat score is originally independent indicator from confusion matrix; however, it is included in confusion matrix in this study because the parameters in confusion matrix are used in this indicator.

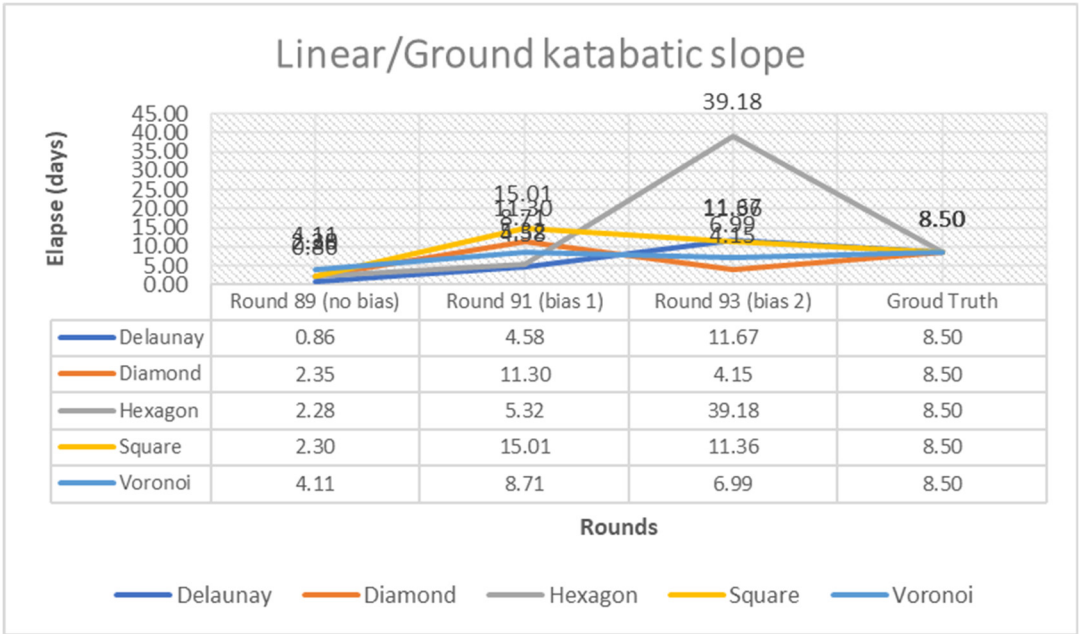

Figure 12: Elapses in the linear/ground katabatic slope (3D) distance for fire isochrone #2.

The closest round in Delaunay and Square is round 93 and the one for other geometries is the round 91.

Table 16: Verification scores with 3D in fire isochrone #2 from five geometries, Delaunay (R93), Diamond (R91), Hexagon (R91), Square (R93) and Voronoi (R91).

Verification method	**Indicator**	**Delaunay**	**Diamond**	**Hexagon**	**Square**	**Voronoi**	**Average score**
Completion Rate [1]		0.29	0.25	0.17	0.28	0.27	0.25
Cohen's Kappa Score	-	0.41	0.45	0.26	0.39	0.44	0.39
	Gap from another slope distance	-0.00	0.00	-0.33	-0.01	0.06	-0.09
Fractions Skill Score (FSS)	-	0.50	0.52	0.32	0.48	0.54	0.47
	Gap from another slope distance	-0.01	-0.01	-0.36	-0.02	0.06	-0.10
Confusion Matrix	Useful	0.50	0.50	0.50	0.50	0.50	0.50
	Accuracy	1.00	1.00	1.00	1.00	1.00	1.00
	Gap from another slope distance	-0.00	0.00	-0.00	-0.00	0.00	-0.00
	Misclassification Rate	0.00	0.00	0.00	0.00	0.00	0.00
	Precision	0.69	0.73	0.44	0.64	0.75	0.65
	Gap from another slope distance	-0.03	0.00	-0.56	-0.02	0.09	-0.15
	Specificity	1.00	1.00	1.00	1.00	1.00	1.00
	Prevalence	0.00	0.00	0.00	0.00	0.00	0.00
	True Positive Rate	0.29	0.32	0.19	0.28	0.32	0.28
	False Positive Rate	0.00	0.00	0.00	0.00	0.00	0.00
	Threat score [2]	0.26	0.29	0.15	0.24	0.29	0.25
	Gap from another slope distance	-0.00	0.00	-0.27	-0.01	0.05	-0.06

[1] Completion Rate is the ratio of total burnt area of prediction against observed data. [2] Threat score is originally independent indicator from confusion matrix; however, it is included in confusion matrix in this study because the parameters in confusion matrix are used in this indicator.

3.2.3. Fire isochrone #3 (ID1548) from 20th till 24th January 2019 (local time)

In experiments, small prediction polygons are employed. The results of elapse are shown below.

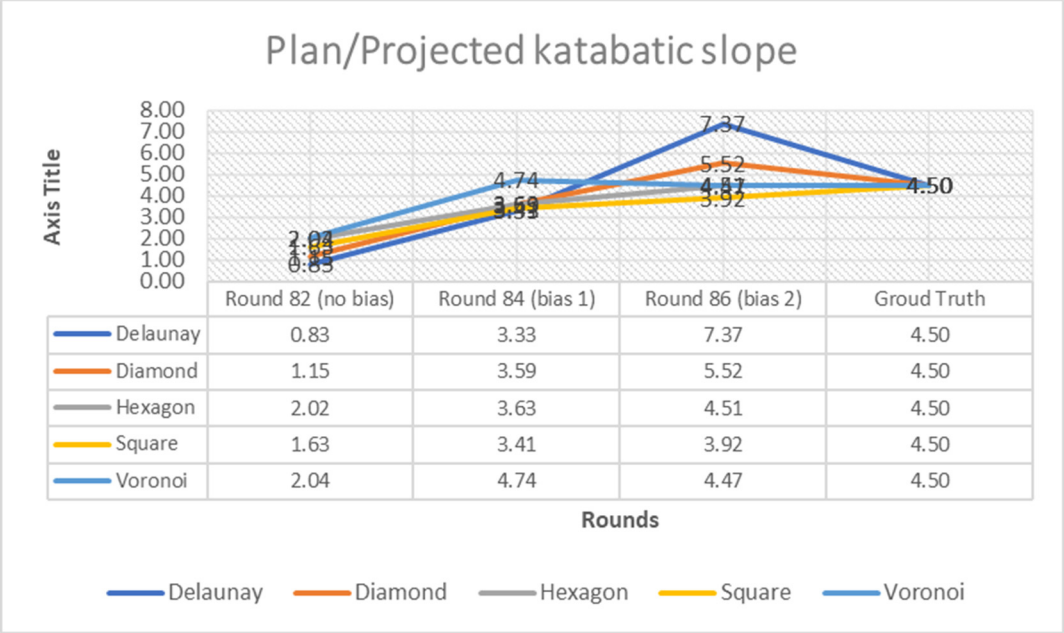

Figure 13: Elapses in the plan/projected katabatic slope (2D) distance for fire isochrone #3.

The closest round in Delaunay and Diamond is round 84 while the one for other geometries is the round 86.

Table 17: Verification scores with 2D in fire isochrone #3 from five geometries, Delaunay (R84), Diamond (R84), Hexagon (R86), Square (R86) and Voronoi (R86).

Verification method	**Indicator**	**Delaunay**	**Diamond**	**Hexagon**	**Square**	**Voronoi**	**Average score**
Completion Rate [1]		1.00	1.00	1.00	1.00	1.00	1.00
Cohen's Kappa Score	-	0.41	0.41	0.30	0.47	0.47	0.41
	Gap from another slope distance	-0.01	-0.01	-0.14	0.03	0.02	-0.02
Fractions Skill Score (FSS)	-	0.48	0.46	0.34	0.55	0.54	0.47
	Gap from another slope distance	-0.03	-0.02	-0.16	0.04	0.01	-0.03
Confusion Matrix	Useful	0.50	0.50	0.50	0.50	0.50	0.50
	Accuracy	1.00	1.00	1.00	1.00	1.00	1.00
	Gap from another slope distance	-0.00	-0.00	-0.00	0.00	0.00	-0.00
	Misclassification Rate	0.00	0.00	0.00	0.00	0.00	0.00
	Precision	0.72	0.72	0.52	0.81	0.81	0.72
	Gap from another slope distance	-0.01	-0.02	-0.24	0.06	0.03	-0.04
	Specificity	1.00	1.00	1.00	1.00	1.00	1.00
	Prevalence	0.00	0.00	0.00	0.00	0.00	0.00
	True Positive Rate	0.29	0.29	0.21	0.33	0.34	0.29
	False Positive Rate	0.00	0.00	0.00	0.00	0.00	0.00
	Threat score [2]	0.26	0.26	0.17	0.31	0.31	0.26
	Gap from another slope distance	-0.01	-0.01	-0.10	0.03	0.02	-0.02

[1] Completion Rate is the ratio of total burnt area of prediction against observed data. [2] Threat score is originally independent indicator from confusion matrix; however, it is included in confusion matrix in this study because the parameters in confusion matrix are used in this indicator.

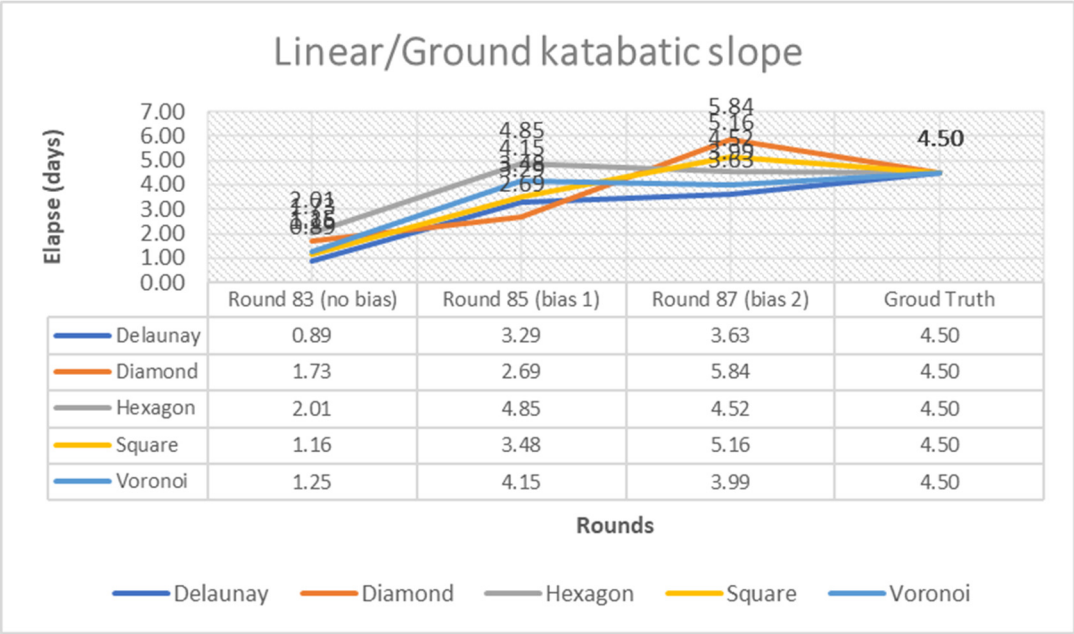

Figure 14: Elapses in the linear/ground katabatic slope (3D) distance for fire isochrone #3.

The closest round in Voronoi is round 85 while the one for other geometries is the round 87.

Table 18: Verification scores with 3D in fire isochrone #3 from five geometries, Delaunay (R87), Diamond (R87), Hexagon (R87), Square (R87) and Voronoi (R85).

Verification method	**Indicator**	**Delaunay**	**Diamond**	**Hexagon**	**Square**	**Voronoi**	**Average score**
Completion Rate [1]		1.00	1.00	1.00	1.00	1.00	1.00
Cohen's Kappa Score	-	0.43	0.43	0.44	0.44	0.46	0.44
	Gap from another slope distance	0.01	0.01	0.06	-0.03	-0.02	0.01
Fractions Skill Score (FSS)	-	0.51	0.48	0.50	0.51	0.53	0.51
	Gap from another slope distance	0.03	0.02	0.07	-0.04	-0.01	0.02
Confusion Matrix	Useful	0.50	0.50	0.50	0.50	0.50	0.50
	Accuracy	1.00	1.00	1.00	1.00	1.00	1.00
	Gap from another slope distance	0.00	0.00	0.00	-0.00	-0.00	0.00
	Misclassification Rate	0.00	0.00	0.00	0.00	0.00	0.00
	Precision	0.73	0.74	0.76	0.75	0.78	0.75

Gap from another slope distance	0.01	0.02	0.11	-0.06	-0.03	0.01
Specificity	1.00	1.00	1.00	1.00	1.00	1.00
Prevalence	0.00	0.00	0.00	0.00	0.00	0.00
True Positive Rate	0.30	0.30	0.31	0.31	0.32	0.31
False Positive Rate	0.00	0.00	0.00	0.00	0.00	0.00
Threat score [2]	0.27	0.27	0.28	0.28	0.30	0.28
Gap from another slope distance	0.01	0.01	0.05	-0.03	-0.02	0.01

[1] Completion Rate is the ratio of total burnt area of prediction against observed data. [2] Threat score is originally independent indicator from confusion matrix; however, it is included in confusion matrix in this study because the parameters in confusion matrix are used in this indicator.

3.3. Simulation of fire propagation by Prototype 2 with resampled data by WindNinja (domain average initialization)

There are several rounds of experiment for each fire isochrone and these sets of rounds are simulated for three fire isochrones. The wind data, which were ingested by the simulator, had been resampled by WindNinja with fine resolution, domain average initialization, and conservation of mass (CoM). In this section, the best fit round is selected in each katabatic slope distance either plan/projected (2D) or linear/ground (3D), geometry among Delaunay, Diamond, Hexagon, Square and Voronoi, and isochrone from #1 to #3.

3.3.1. Fire isochrone #1 (ID1499) from 18th till 22nd January 2019 (local time)

In experiments, small prediction polygons are employed. The results of elapse are shown below.

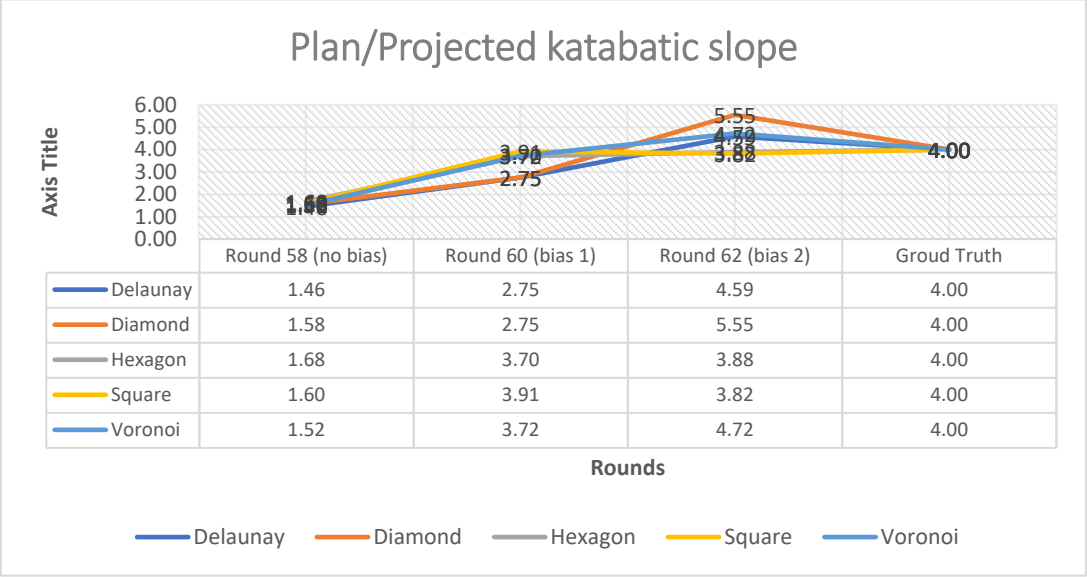

Figure 15: Elapses in the plan/projected katabatic slope (2D) distance for fire isochrone #1.

The closest round in Delaunay and Hexagon is round 62 while the one for other geometries is the round 60.

Table 19: Verification scores with 2D in fire isochrone #1 from five geometries, Delaunay (R62), Diamond (R60), Hexagon (R62), Square (R60) and Voronoi (R60).

Verification method	**Indicator**	**Delaunay**	**Diamond**	**Hexagon**	**Square**	**Voronoi**	**Average score**

Cohen's Kappa Score	-	0.62	0.67	0.65	0.55	0.57	0.61
	Gap from another slope distance	0.13	0.02	0.31	-0.07	0.02	0.08
Fractions Skill Score (FSS)	-	0.71	0.73	0.72	0.65	0.66	0.69
	Gap from another slope distance	0.14	0.00	0.32	-0.07	0.01	0.08
Confusion Matrix	Useful	0.50	0.50	0.50	0.50	0.50	0.50
	Accuracy	1.00	1.00	1.00	1.00	1.00	1.00
	Gap from another slope distance	0.00	0.00	0.00	-0.00	0.00	0.00
	Misclassification Rate	0.00	0.00	0.00	0.00	0.00	0.00
	Precision	0.80	0.86	0.84	0.69	0.73	0.78
	Gap from another slope distance	0.17	0.03	0.39	-0.08	0.02	0.11
	Specificity	1.00	1.00	1.00	1.00	1.00	1.00
	Prevalence	0.00	0.00	0.00	0.00	0.00	0.00
	True Positive Rate	0.50	0.55	0.53	0.46	0.47	0.50
	False Positive Rate	0.00	0.00	0.00	0.00	0.00	0.00
	Threat score [1]	0.45	0.51	0.48	0.38	0.40	0.45
	Gap from another slope distance	0.12	0.02	0.27	-0.07	0.02	0.08

[1] Threat score is originally independent indicator from confusion matrix; however, it is included in confusion matrix in this study because the parameters in confusion matrix are used in this indicator.

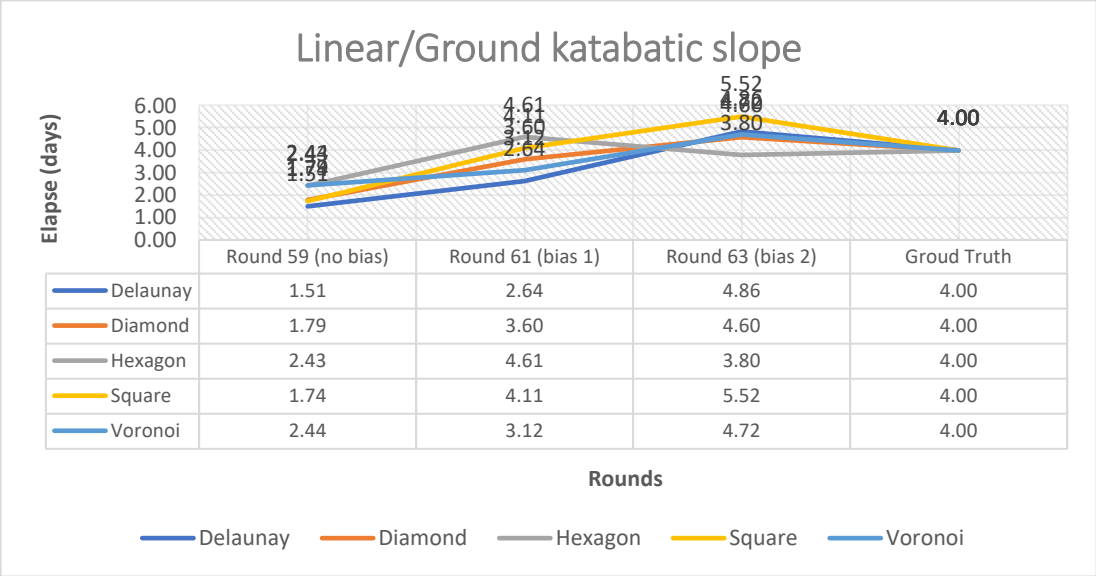

Figure 16: Elapses in the linear/ground katabatic slope (3D) distance for fire isochrone #6.

The closest round in Diamond and Square is round 61 while the one for other geometries is the round 63.

Table 20: Verification scores with 3D in fire isochrone #5 from five geometries, Delaunay (R63), Diamond (R61), Hexagon (R63), Square (R61) and Voronoi (R63).

Verification method	Indicator	Delaunay	Diamond	Hexagon	Square	Voronoi	Average score
Cohen's Kappa Score	-	0.48	0.65	0.35	0.62	0.56	0.53
	Gap from another slope distance	-0.13	-0.02	-0.31	0.07	-0.02	-0.08
Fractions Skill Score (FSS)	-	0.57	0.73	0.40	0.72	0.65	0.61
	Gap from another slope distance	-0.14	-0.00	-0.32	0.07	-0.01	-0.08
Confusion Matrix	Useful	0.50	0.50	0.50	0.50	0.50	0.50
	Accuracy	1.00	1.00	1.00	1.00	1.00	1.00
	Gap from another slope distance	-0.00	-0.00	-0.00	0.00	-0.00	-0.00
	Misclassification Rate	0.00	0.00	0.00	0.00	0.00	0.00
	Precision	0.62	0.84	0.45	0.77	0.71	0.68
	Gap from another slope distance	-0.17	-0.03	-0.39	0.08	-0.02	-0.11
	Specificity	1.00	1.00	1.00	1.00	1.00	1.00
	Prevalence	0.00	0.00	0.00	0.00	0.00	0.00
	True Positive Rate	0.40	0.53	0.28	0.51	0.46	0.44
	False Positive Rate	0.00	0.00	0.00	0.00	0.00	0.00
	Threat score [1]	0.32	0.48	0.21	0.45	0.39	0.37
	Gap from another slope distance	-0.12	-0.02	-0.27	0.07	-0.02	-0.08

[1] Threat score is originally independent indicator from confusion matrix; however, it is included in confusion matrix in this study because parameters in confusion matrix are used in this indicator.

3.3.2. Fire isochrone #2 (ID1547) from 16th till 24th January 2019 (local time)

In experiments, small prediction polygons are employed. The results of elapse are shown below.

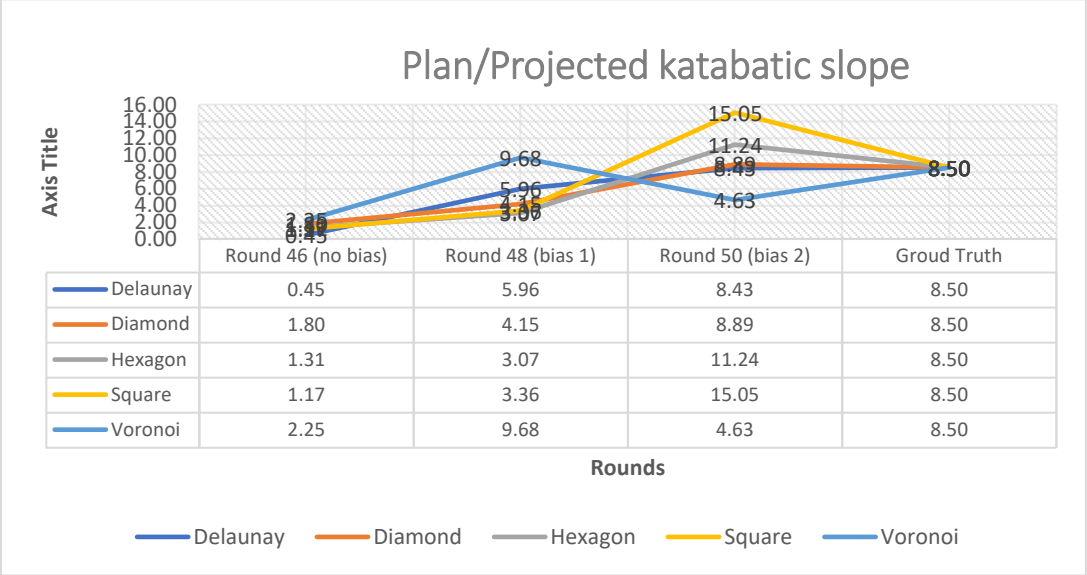

Figure 17: Elapses in the plan/projected katabatic slope (2D) distance for fire isochrone #2.

The closest round in Square and Voronoi is round 48 while the one for other geometries is the round 50.

Table 21: Verification scores with 2D in fire isochrone #4 from five geometries, Delaunay (R50), Diamond (R50), Hexagon (R50), Square (R48) and Voronoi (R48).

Verification method	**Indicator**	**Delaunay**	**Diamond**	**Hexagon**	**Square**	**Voronoi**	**Average score**
Cohen's Kappa Score	-	0.51	0.22	0.48	0.30	0.47	0.39
	Gap from another slope distance	0.09	-0.36	0.10	-0.11	0.17	0.06
Fractions Skill Score (FSS)	-	0.62	0.26	0.57	0.38	0.56	0.48
	Gap from another slope distance	0.09	-0.40	0.12	-0.12	0.19	0.08
Confusion Matrix	Useful	0.50	0.50	0.50	0.50	0.50	0.50
	Accuracy	1.00	1.00	1.00	1.00	1.00	1.00
	Gap from another slope distance	0.00	-0.00	0.00	-0.00	0.00	0.00
	Misclassification Rate	0.00	0.00	0.00	0.00	0.00	0.00
	Precision	0.87	0.35	0.81	0.48	0.80	0.66
	Gap from another slope distance	0.16	-0.58	0.17	-0.18	0.26	
	Specificity	1.00	1.00	1.00	1.00	1.00	1.00
	Prevalence	0.00	0.00	0.00	0.00	0.00	0.00
	True Positive Rate	0.36	0.16	0.34	0.21	0.34	0.28
	False Positive Rate	0.00	0.00	0.00	0.00	0.00	0.00
	Threat score [1]	0.34	0.12	0.32	0.17	0.31	0.24
	Gap from another slope distance	0.08	-0.28	0.08	-0.08	0.13	0.03

[1] Threat score is originally independent indicator from confusion matrix; however, it is included in confusion matrix in this study because parameters in confusion matrix are used in this indicator.

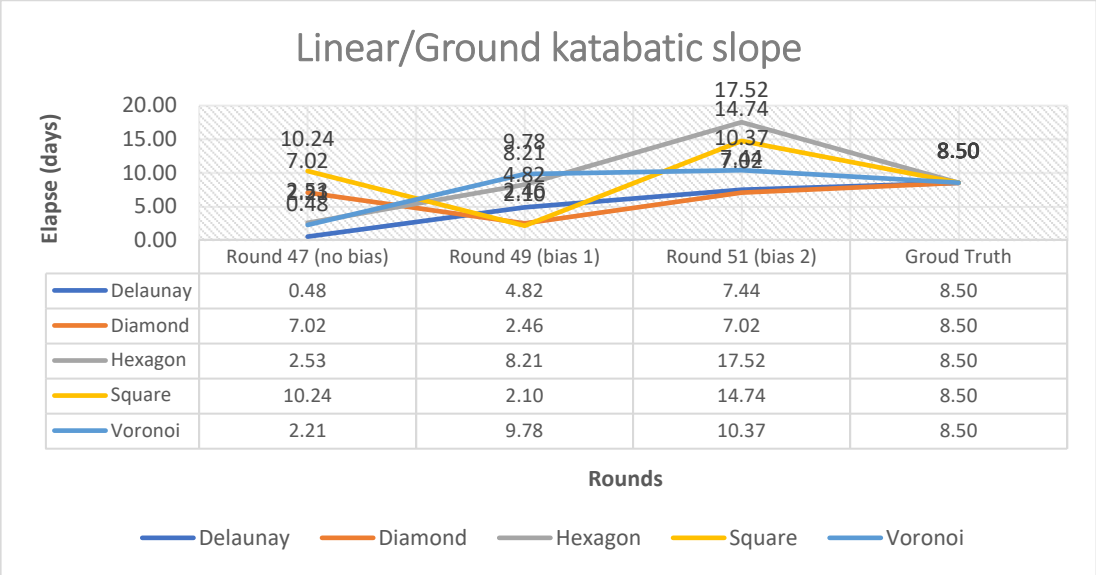

Figure 18: Elapses in the linear/ground katabatic slope (3D) distance for fire isochrone #2.

The closest rounds are 51, 47, 49, 47 and 49 in Delaunay, Diamond, Hexagon, Square and Voronoi respectively.

Table 22: Verification scores with 3D in fire isochrone #4 from five geometries, Delaunay (R51), Diamond (R47), Hexagon (R49), Square (R47) and Voronoi (R49).

Verification method	**Indicator**	**Delaunay**	**Diamond**	**Hexagon**	**Square**	**Voronoi**	**Average score**
Cohen's Kappa Score	-	0.42	0.33	0.38	0.22	0.31	0.33
	Gap from another slope distance	-0.09	-0.09	-0.10	-0.26	-0.17	-0.06
Fractions Skill Score (FSS)	-	0.53	0.41	0.45	0.26	0.37	0.40
	Gap from another slope distance	-0.09	-0.10	-0.12	-0.35	-0.19	-0.19
Confusion Matrix	Useful	0.50	0.50	0.50	0.50	0.50	0.50
	Accuracy	1.00	1.00	1.00	1.00	1.00	1.00
	Gap from another slope distance	-0.00	-0.00	-0.00	-0.00	-0.00	-0.00
	Misclassification Rate	0.00	0.00	0.00	0.00	0.00	0.00
	Precision	0.72	0.55	0.64	1.00	0.54	0.69
	Gap from another slope distance	-0.16	-0.15	-0.17	0.21	-0.26	0.03
	Specificity	1.00	1.00	1.00	1.00	1.00	1.00
	Prevalence	0.00	0.00	0.00	0.00	0.00	0.00
	True Positive Rate	0.29	0.24	0.27	0.12	0.21	0.23
	False Positive Rate	0.00	0.00	0.00	0.00	0.00	0.00
	Threat score [1]	0.26	0.20	0.24	0.12	0.18	0.21

	Gap from another slope distance	-0.08	-0.07	-0.08	-0.19	-0.13	-0.03

[1] Threat score is originally independent indicator from confusion matrix; however, it is included in confusion matrix in this study because parameters in confusion matrix are used in this indicator.

3.3.3. Fire isochrone #3 (ID1548) from 20th till 24th January 2019 (local time)

In experiments, small prediction polygons are employed. The results of elapse are shown below.

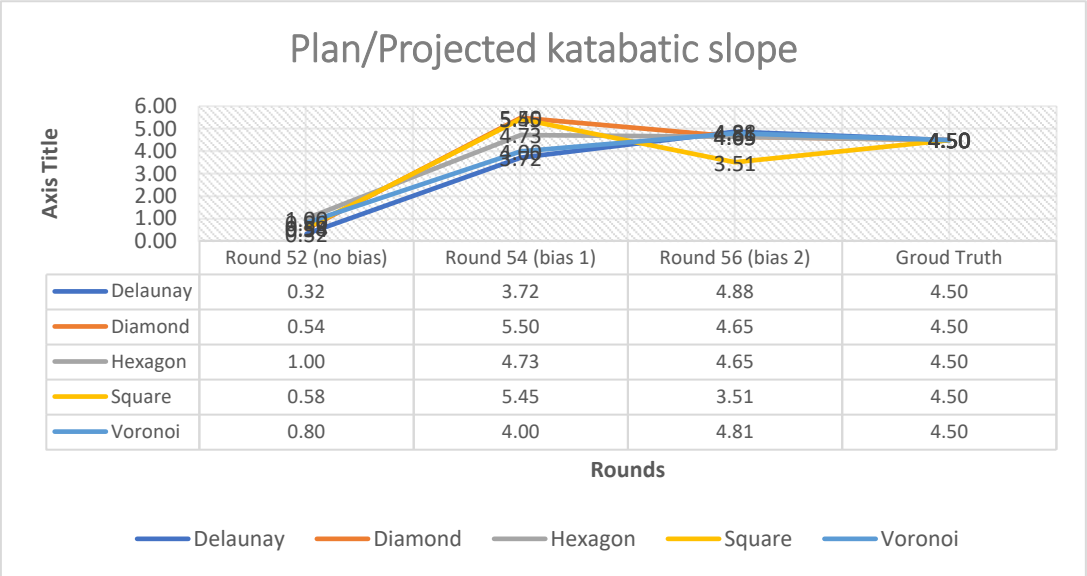

Figure 19: Elapses in the plan/projected katabatic slope (2D) distance for fire isochrone #3.

The closest round in Square is round 54 while the one for other geometries is the round 56.

Table 23: Verification scores with 2D in fire isochrone #5 from five geometries, Delaunay (R56), Diamond (R56), Hexagon (R56), Square (R54) and Voronoi (R56).

Verification method	**Indicator**	**Delaunay**	**Diamond**	**Hexagon**	**Square**	**Voronoi**	**Average score**
Cohen's Kappa Score	-	0.35	0.42	0.47	0.45	0.22	0.38
	Gap from another slope distance	-0.08	0.05	0.07	0.00	-0.23	-0.04
Fractions Skill Score (FSS)	-	0.42	0.48	0.53	0.52	0.25	0.44
	Gap from another slope distance	-0.08	0.04	0.09	-0.01	-0.27	-0.05
Confusion Matrix	Useful	0.50	0.50	0.50	0.50	0.50	0.50
	Accuracy	1.00	1.00	1.00	1.00	1.00	1.00
	Gap from another slope distance	-0.00	0.00	0.00	0.00	-0.00	-0.00
	Misclassification Rate	0.00	0.00	0.00	0.00	0.00	0.00
	Precision	0.62	0.74	0.82	0.77	0.38	0.66

	Gap from another slope distance	-0.12	0.09	0.12	0.00	-0.39	-0.06
	Specificity	1.00	1.00	1.00	1.00	1.00	1.00
	Prevalence	0.00	0.00	0.00	0.00	0.00	0.00
	True Positive Rate	0.24	0.30	0.33	0.32	0.15	0.27
	False Positive Rate	0.00	0.00	0.00	0.00	0.00	0.00
	Threat score [1]	0.21	0.27	0.31	0.29	0.12	0.24
	Gap from another slope distance	-0.06	0.04	0.06	0.00	-0.17	-0.02

[1] Threat score is originally independent indicator from confusion matrix; however, it is included in confusion matrix in this study because the parameters in confusion matrix are used in this indicator.

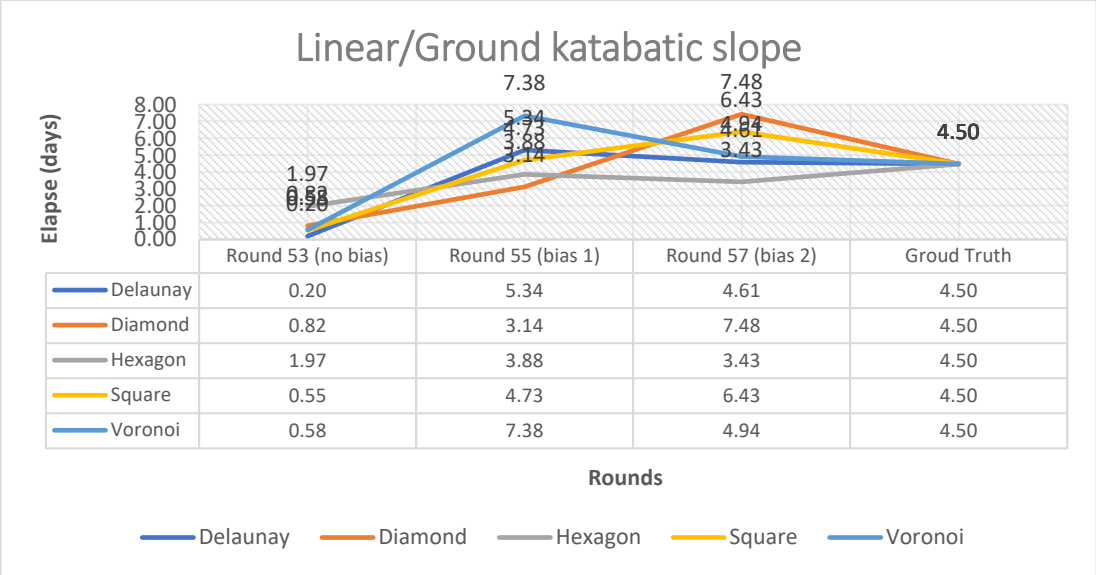

Figure 20: Elapses in the linear/ground katabatic slope (3D) distance for fire isochrone #3.

The closest round in Delaunay and Voronoi is round 57 while the one for other geometries is the round 55.

Table 24: Verification scores with 3D in fire isochrone #5 from five geometries, Delaunay (R57), Diamond (R55), Hexagon (R55), Square (R55) and Voronoi (R57).

Verification method	**Indicator**	**Delaunay**	**Diamond**	**Hexagon**	**Square**	**Voronoi**	**Average score**
Cohen's Kappa Score	-	0.42	0.37	0.40	0.45	0.45	0.42
	Gap from another slope distance	0.08	-0.05	-0.07	0.00	0.23	0.04
Fractions Skill Score (FSS)	-	0.50	0.44	0.45	0.53	0.52	0.49
	Gap from another slope distance	0.08	-0.04	-0.09	0.01	0.27	0.05
	Useful	0.50	0.50	0.50	0.50	0.50	0.50

Confusion Matrix	Accuracy	1.00	1.00	1.00	1.00	1.00	1.00
	Gap from another slope distance	0.00	-0.00	-0.00	0.00	0.00	0.00
	Misclassification Rate	0.00	0.00	0.00	0.00	0.00	0.00
	Precision	0.73	0.65	0.70	0.77	0.77	0.73
	Gap from another slope distance	0.12	-0.09	-0.12	0.00	0.39	0.06
	Specificity	1.00	1.00	1.00	1.00	1.00	1.00
	Prevalence	0.00	0.00	0.00	0.00	0.00	0.00
	True Positive Rate	0.30	0.26	0.28	0.32	0.32	0.30
	False Positive Rate	0.00	0.00	0.00	0.00	0.00	0.00
	Threat score [1]	0.27	0.23	0.25	0.29	0.29	0.26
	Gap from another slope distance	0.06	-0.04	-0.06	0.00	0.17	0.02

[1] Threat score is originally independent indicator from confusion matrix; however, it is included in confusion matrix in this study because parameters in confusion matrix are used in this indicator.

3.4. Simulation of fire propagation by Prototype 2 with resampled data by WindNinja (grid initialization)

Three rounds of experiment for fire isochrone #1, #2 and #3 were simulated by ingesting resampled wind filed by WindNinja. Each area of these area is less than $10km^2$. The motivation of the simulation with the finer resolution and higher topographically sensitivity than the those of BARRA-TA. The wind fields are resampled from gridded wind fields, whose resolution is the same as BARRA-TA, by using options, gridded initialization, conservation of mass (CoM) and fine resolution. Therefore, the resampled wind was expected to account for both topography and vertical atmospheric interaction.

3.4.1. Fire isochrone #1 (ID1499) from 18th till 22nd January 2019 (local time)

In experiments, small prediction polygons are employed. The results of elapse are shown below.

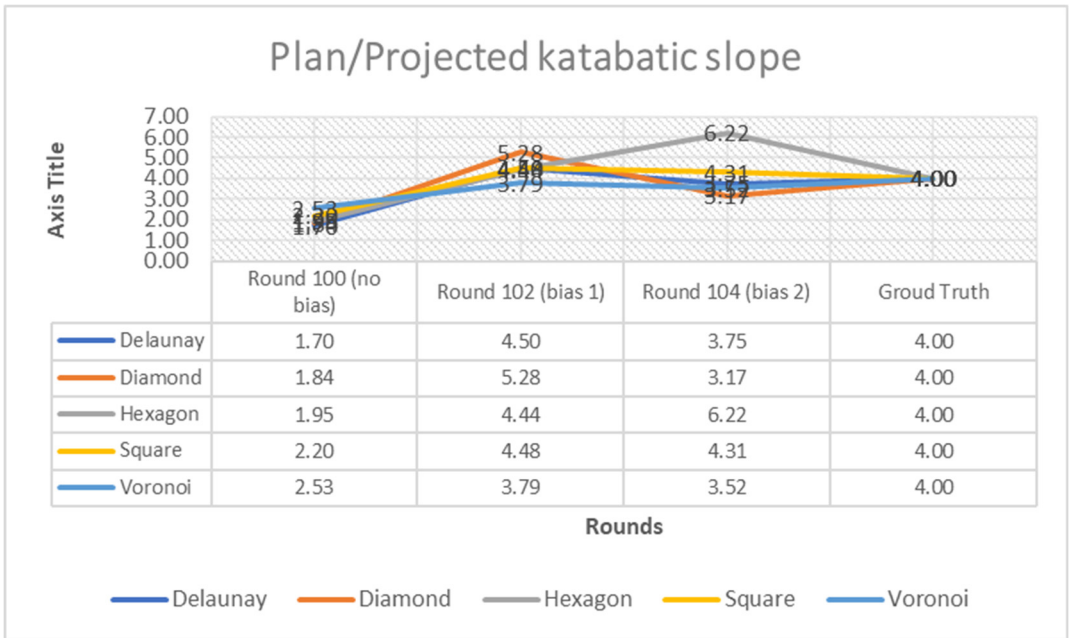

Figure 21: Elapses in the plan/projected katabatic slope (2D) distance for fire isochrone #1.

The closest round in Hexagon and Voronoi is round 102 while the one for other geometries is the round 104.

Table 25: Verification scores with 2D in fire isochrone #1 from five geometries, Delaunay (R104), Diamond (R104), Hexagon (R102), Square (R104) and Voronoi (R102).

Verification method	**Indicator**	**Delaunay**	**Diamond**	**Hexagon**	**Square**	**Voronoi**	**Average score**
Completion Rate [1]		1.00	1.00	1.00	1.00	1.00	1.00
Cohen's Kappa Score	-	0.59	0.58	0.59	0.54	0.61	0.58
	Gap from another slope distance	0.07	0.01	0.11	0.03	0.12	0.07
Fractions Skill Score (FSS)	-	0.68	0.65	0.66	0.62	0.70	0.66
	Gap from another slope distance	0.07	0.01	0.12	0.03	0.13	0.07
Confusion Matrix	Useful	0.50	0.50	0.50	0.50	0.50	0.50
	Accuracy	1.00	1.00	1.00	1.00	1.00	1.00
	Gap from another slope distance	0.00	0.00	0.00	0.00	0.00	0.00
	Misclassification Rate	0.00	0.00	0.00	0.00	0.00	0.00
	Precision	0.78	0.75	0.76	0.67	0.78	0.75
	Gap from another slope distance	0.10	0.01	0.15	0.03	0.17	0.09
	Specificity	1.00	1.00	1.00	1.00	1.00	1.00
	Prevalence	0.00	0.00	0.00	0.00	0.00	0.00
	True Positive Rate	0.48	0.48	0.48	0.45	0.50	0.48
	False Positive Rate	0.00	0.00	0.00	0.00	0.00	0.00
	Threat score [2]	0.42	0.41	0.42	0.37	0.44	0.41
	Gap from another slope distance	0.07	0.01	0.11	0.02	0.12	0.06

[1] Completion Rate is the ratio of total burnt area of prediction against observed data. [2] Threat score is originally independent indicator from confusion matrix; however, it is included in confusion matrix in this study because the parameters in confusion matrix are used in this indicator.

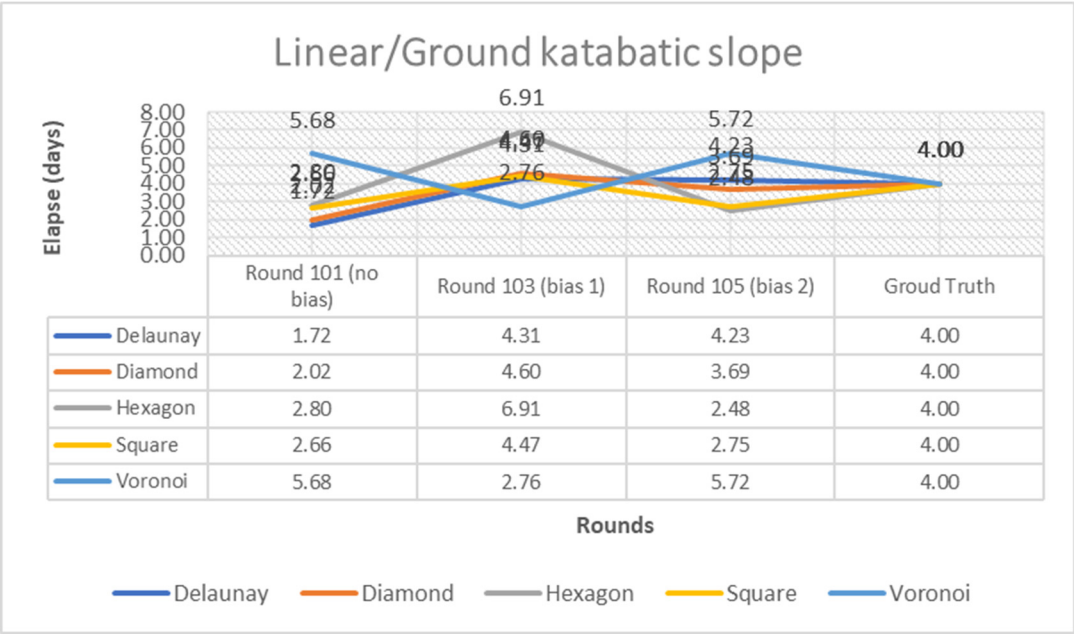

Figure 22: Elapses in the linear/ground katabatic slope (3D) distance for fire isochrone #1.

The closest rounds in Delaunay, Diamond, Hexagon, Square and Voronoi are 105, 105, 101, 103, and 103 respectively.

Table 26: Verification scores with 3D in fire isochrone #2 from five geometries, Delaunay (R105), Diamond (R105), Hexagon (R101), Square (R103) and Voronoi (R103).

Verification method	**Indicator**	**Delaunay**	**Diamond**	**Hexagon**	**Square**	**Voronoi**	**Average score**
Completion Rate [1]		1.00	1.00	1.00	1.00	1.00	1.00
Cohen's Kappa Score	-	0.52	0.58	0.47	0.51	0.48	0.51
	Gap from another slope distance	-0.07	-0.01	-0.11	-0.03	-0.12	-0.07
Fractions Skill Score (FSS)	-	0.61	0.64	0.54	0.59	0.58	0.59
	Gap from another slope distance	-0.07	-0.01	-0.12	-0.03	-0.13	-0.07
Confusion Matrix	Useful	0.50	0.50	0.50	0.50	0.50	0.50
	Accuracy	1.00	1.00	1.00	1.00	1.00	1.00
	Gap from another slope distance	-0.00	-0.00	-0.00	-0.00	-0.00	-0.00
	Misclassification Rate	0.00	0.00	0.00	0.00	0.00	0.00
	Precision	0.68	0.74	0.61	0.64	0.61	0.66
	Gap from another slope distance	-0.10	-0.01	-0.15	-0.03	-0.17	-0.09
	Specificity	1.00	1.00	1.00	1.00	1.00	1.00
	Prevalence	0.00	0.00	0.00	0.00	0.00	0.00
	True Positive Rate	0.42	0.47	0.39	0.43	0.40	0.42
	False Positive Rate	0.00	0.00	0.00	0.00	0.00	0.00
	Threat score [2]	0.35	0.41	0.31	0.34	0.32	0.35

	Gap from another slope distance	-0.07	-0.01	-0.11	-0.02	-0.12	-0.06

[1] Completion Rate is the ratio of total burnt area of prediction against observed data. [2] Threat score is originally independent indicator from confusion matrix; however, it is included in confusion matrix in this study because the parameters in confusion matrix are used in this indicator.

3.4.2. Fire isochrone #2 (ID1547) from 16th till 24th January 2019 (local time)

In experiments, small prediction polygons are employed. The results of elapse are shown below.

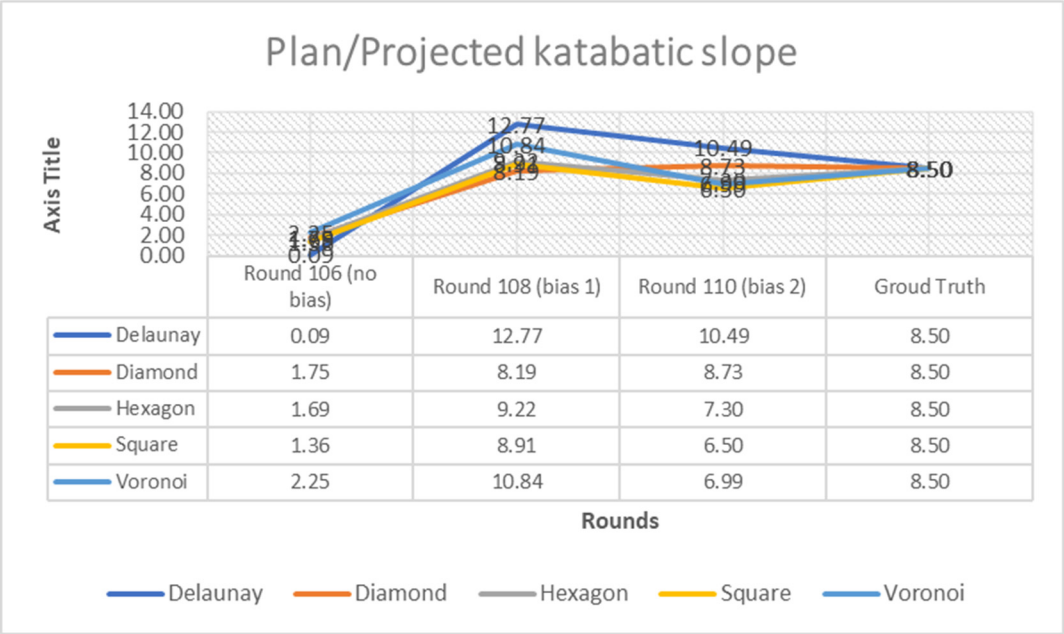

Figure 23: Elapses in the plan/projected katabatic slope (2D) distance for fire isochrone #2.

The closest rounds in Delaunay, Diamond, Hexagon, Square and Voronoi are the round 110, 110, 108, 108 and 110 respectively.

Table 27: Verification scores with 2D in fire isochrone #2 from five geometries, Delaunay (R110), Diamond (R108), Hexagon (R110), Square (R108) and Voronoi (R110).

Verification method	**Indicator**	**Delaunay**	**Diamond**	**Hexagon**	**Square**	**Voronoi**	**Average score**
Completion Rate [1]		1.00	1.00	1.01	1.01	1.00	1.00
Cohen's Kappa Score	-	0.33	0.25	0.51	0.47	0.40	0.39
	Gap from another slope distance	-0.16	-0.14	-0.06	0.03	0.13	-0.04
Fractions Skill Score (FSS)	-	0.42	0.31	0.60	0.59	0.48	0.48
	Gap from another slope distance	-0.17	-0.15	-0.07	0.04	0.14	-0.04

Confusion Matrix	Useful	0.50	0.50	0.50	0.50	0.50	0.50
	Accuracy	1.00	1.00	1.00	1.00	1.00	1.00
	Gap from another slope distance	-0.00	-0.00	-0.00	0.00	0.00	-0.00
	Misclassification Rate	0.00	0.00	0.00	0.00	0.00	0.00
	Precision	0.57	0.41	0.85	0.78	0.68	0.66
	Gap from another slope distance	-0.27	-0.23	-0.10	0.05	0.22	-0.06
	Specificity	1.00	1.00	1.00	1.00	1.00	1.00
	Prevalence	0.00	0.00	0.00	0.00	0.00	0.00
	True Positive Rate	0.24	0.18	0.36	0.34	0.28	0.28
	False Positive Rate	0.00	0.00	0.00	0.00	0.00	0.00
	Threat score [2]	0.20	0.14	0.34	0.31	0.25	0.23
	Gap from another slope distance	-0.12	-0.10	-0.05	0.03	0.09	-0.05

[1] Completion Rate is the ratio of total burnt area of prediction against observed data. [2] Threat score is originally independent indicator from confusion matrix; however, it is included in confusion matrix in this study because the parameters in confusion matrix are used in this indicator.

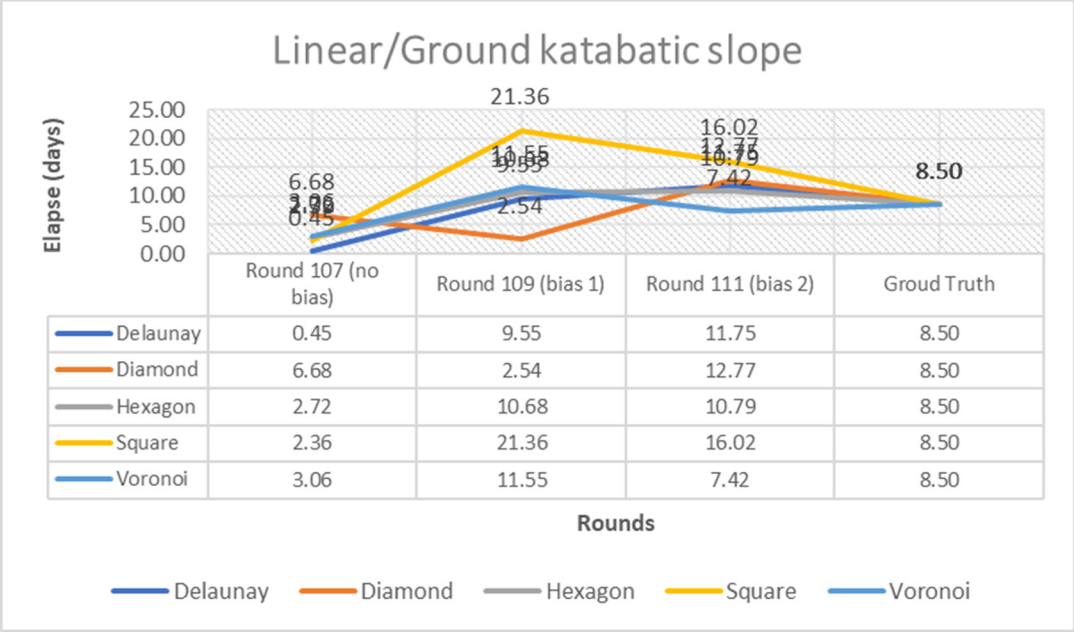

Figure 24: Elapses in the linear/ground katabatic slope (3D) distance for fire isochrone #2.

The closest rounds in Delaunay, Diamond, Hexagon, Square and Voronoi are the round 109, 107, 109, 107 and 111 respectively.

Table 28: Verification scores with 3D in fire isochrone #2 from five geometries, Delaunay (R109), Diamond (R107), Hexagon (R109), Square (R107) and Voronoi (R111).

Verification method	**Indicator**	**Delaunay**	**Diamond**	**Hexagon**	**Square**	**Voronoi**	**Average score**
Completion Rate [1]		1.00	0.11	1.01	0.46	1.01	0.72
Cohen's Kappa Score	-	0.49	0.39	0.57	0.44	0.27	0.43
	Gap from another slope distance	0.16	-0.18	0.06	-0.04	-0.13	0.04

Fractions Skill Score (FSS)	-	0.60	0.46	0.66	0.55	0.34	0.52
	Gap from another slope distance	0.17	-0.21	0.07	-0.04	-0.14	0.04
Confusion Matrix	Useful	0.50	0.50	0.50	0.50	0.50	0.50
	Accuracy	1.00	1.00	1.00	1.00	1.00	1.00
	Gap from another slope distance	0.00	-0.00	0.00	-0.00	-0.00	0.00
	Misclassification Rate	0.00	0.00	0.00	0.00	0.00	0.00
	Precision	0.84	0.64	0.95	0.73	0.46	0.72
	Gap from another slope distance	0.27	-0.29	0.10	-0.07	-0.22	0.06
	Specificity	1.00	1.00	1.00	1.00	1.00	1.00
	Prevalence	0.00	0.00	0.00	0.00	0.00	0.00
	True Positive Rate	0.35	0.28	0.40	0.32	0.19	0.31
	False Positive Rate	0.00	0.00	0.00	0.00	0.00	0.00
	Threat score [2]	0.33	0.24	0.39	0.29	0.16	0.28
	Gap from another slope distance	0.12	-0.15	0.05	-0.04	-0.09	0.05

[1] Completion Rate is the ratio of total burnt area of prediction against observed data. [2] Threat score is originally independent indicator from confusion matrix; however, it is included in confusion matrix in this study because the parameters in confusion matrix are used in this indicator.

3.4.3. Fire isochrone #3 (ID1548) from 20th till 24th January 2019 (local time)

In experiments, small prediction polygons are employed. The results of elapse are shown below.

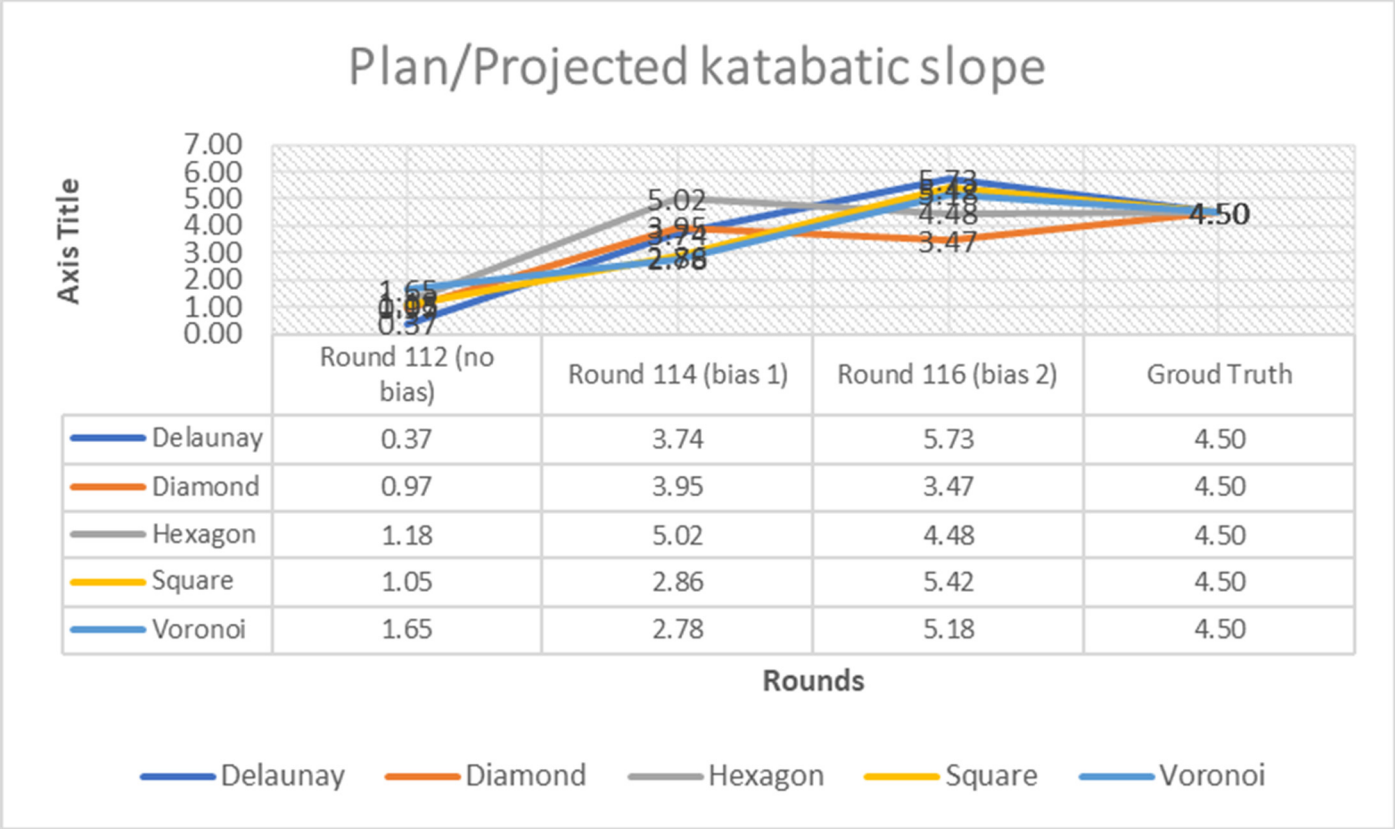

Figure 25: Elapses in the plan/projected katabatic slope (2D) distance for fire isochrone #3.

The closest round in Delaunay and Diamond is 114 while the one for other geometries is the round 116.

Table 29: Verification scores with 2D in fire isochrone #3 from five geometries, Delaunay (R114), Diamond (R114), Hexagon (R116), Square (R116) and Voronoi (R116).

Verification method	**Indicator**	**Delaunay**	**Diamond**	**Hexagon**	**Square**	**Voronoi**	**Average score**
Completion Rate [1]		1.00	1.00	1.00	1.00	1.00	1.00
Cohen's Kappa Score	-	0.33	0.27	0.51	0.42	0.39	0.38
	Gap from another slope distance	-0.06	-0.14	0.07	0.06	-0.06	-0.03
Fractions Skill Score (FSS)	-	0.41	0.31	0.56	0.50	0.45	0.45
	Gap from another slope distance	-0.05	-0.17	0.07	0.09	-0.07	-0.03
Confusion Matrix	Useful	0.50	0.50	0.50	0.50	0.50	0.50
	Accuracy	1.00	1.00	1.00	1.00	1.00	1.00
	Gap from another slope distance	-0.00	-0.00	0.00	0.00	-0.00	-0.00
	Misclassification Rate	0.00	0.00	0.00	0.00	0.00	0.00
	Precision	0.58	0.48	0.88	0.72	0.67	0.66
	Gap from another slope distance	-0.11	-0.25	0.12	0.11	-0.11	-0.05
	Specificity	1.00	1.00	1.00	1.00	1.00	1.00
	Prevalence	0.00	0.00	0.00	0.00	0.00	0.00
	True Positive Rate	0.23	0.19	0.35	0.30	0.27	0.27

	False Positive Rate	0.00	0.00	0.00	0.00	0.00	0.00
	Threat score [2]	0.20	0.16	0.34	0.27	0.24	0.22
	Gap from another slope distance	-0.04	-0.11	0.06	0.05	-0.05	-0.03

[1] Completion Rate is the ratio of total burnt area of prediction against observed data. [2] Threat score is originally independent indicator from confusion matrix; however, it is included in confusion matrix in this study because the parameters in confusion matrix are used in this indicator.

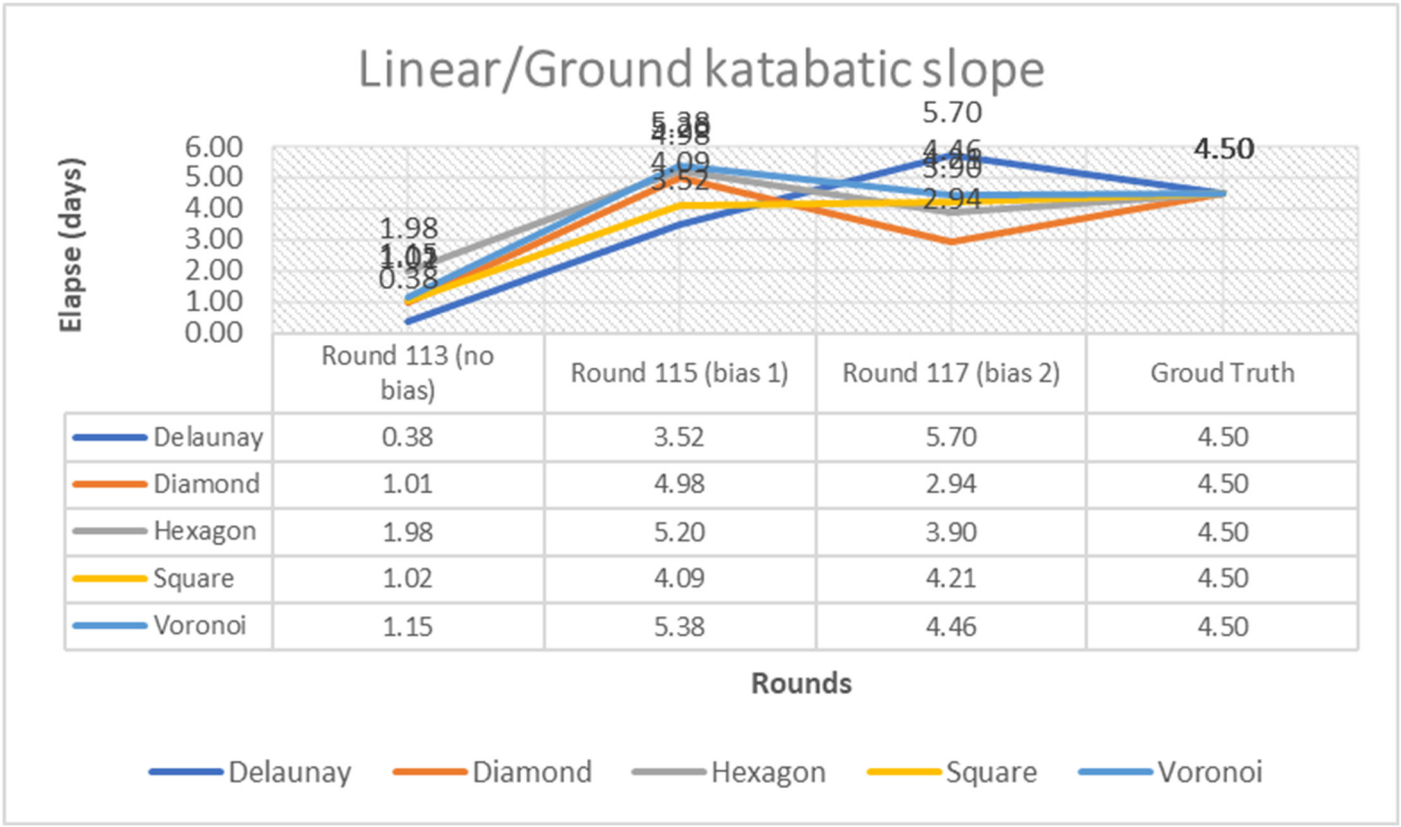

Figure 26: Elapses in the linear/ground katabatic slope (3D) distance for fire isochrone #3.

The closest round in Delaunay and Diamond is 115 while the one for other geometries is the round 115.

Table 30: Verification scores with 3D in fire isochrone #3 from five geometries, Delaunay (R115), Diamond (R115), Hexagon (R117), Square (R117) and Voronoi (R117).

Verification method	**Indicator**	**Delaunay**	**Diamond**	**Hexagon**	**Square**	**Voronoi**	**Average score**
Completion Rate [1]		1.00	1.00	1.00	1.00	1.00	1.00
	-	0.39	0.42	0.44	0.36	0.45	0.41

Cohen's Kappa Score	*Gap from another slope distance*	0.06	0.14	-0.07	-0.06	0.06	0.03
Fractions Skill Score (FSS)	-	0.46	0.48	0.49	0.41	0.52	0.47
	Gap from another slope distance	0.05	0.17	-0.07	-0.09	0.07	0.03
Confusion Matrix	Useful	0.50	0.50	0.50	0.50	0.50	0.50
	Accuracy	1.00	1.00	1.00	1.00	1.00	1.00
	Gap from another slope distance	0.00	0.00	-0.00	-0.00	0.00	0.00
	Misclassification Rate	0.00	0.00	0.00	0.00	0.00	0.00
	Precision	0.69	0.73	0.76	0.61	0.77	0.71
	Gap from another slope distance	0.11	0.25	-0.12	-0.11	0.11	0.05
	Specificity	1.00	1.00	1.00	1.00	1.00	1.00
	Prevalence	0.00	0.00	0.00	0.00	0.00	0.00
	True Positive Rate	0.27	0.29	0.31	0.25	0.32	0.29
	False Positive Rate	0.00	0.00	0.00	0.00	0.00	0.00
	Threat score [2]	0.24	0.26	0.28	0.22	0.29	0.26
	Gap from another slope distance	0.04	0.11	-0.06	-0.05	0.05	0.03

[1] Completion Rate is the ratio of total burnt area of prediction against observed data. [2] Threat score is originally independent indicator from confusion matrix; however, it is included in confusion matrix in this study because the parameters in confusion matrix are used in this indicator.

4. Analysis

4.1. Fire simulation and ruggedness of terrains

Rugged terrain shows the more occurrence of conducive structures and lower simulation score than the mild terrains. Fires were simulated with three types of wind. The first is the surface wind from BARRA-TA. The second is the resampled wind by WindNinja with domain average initialization (WN-DAI). The third is the resampled data by WindNinja with gridded initialization (WN-GI). Three fire isochrones are employed as the observed fire, each of which is less than $10km^2$. Isochrone #1 and #2, are located in rugged terrain while #3 is in the less rugged terrain. The simulation scores are represented by the fractions skill score (FSS) which is the greater than its usefulness. There are who tendencies. One is that the more rugged the terrain is, the more conducive structures were observed, and the less simulation score was. Another tendency is that all the simulation with the resampled wind show lower score than the ones with crude wind.

Table 31: Comparison of fractions skill score (FSS) with BARRA-TA and the resampled wind field by WindNinja.

Fire isochrone #	BARRA-TA	WN-DAI	WN-GI	Conducive structures (%)	Elevation gap
1	8	9	10	6.51	335
2	7	4	5	11.56	571
3	5	4	2	40.15	619

Below tables shows the median value of main indicators. Tendency is that the scores with the resampled winds with domain average initialization (WN-DAI) is slightly higher than other types of wind in fire isochrone #1. On the other hand, BARRA-TA shows the best in isochrone #2 and #3. Exception is the accuracy in confusion matrix. it shows nearly 1.00 in all fire isochrones because the total areas, which present in both numerator and denominator to calculate accuracy, are significantly larger than isochrones.

Table 32: Median of **Fractions Skill Score**. Comparison of fire simulations using between BARRA-TA and the resampled winds field by WindNinja.

Fire isochrone #	BARRA-TA	WN-DAI	WN-GI
1	0.67	0.68	0.63
2	0.52	0.43	0.51
3	0.50	0.49	0.47

Table 33: Median of **Cohen's Kappa**: Comparison of fire simulations using between BARRA-TA and the resampled wind field by WindNinja. All scores fall on to "moderate" (between 0.41 and 0.60) apart from the ones with WN-DAI on fire isochrone #2, which is categorized in "far" (between 0.21 and 0.40) [18].

Fire isochrone #	BARRA-TA	WN-DAI	WN-GI
1	0.58	0.60	0.56
2	0.43	0.36	0.42
3	0.43	0.42	0.40

Table 34: Median of **Accuracy**: Comparison of fire simulations using between BARRA-TA and the resampled wind field by WindNinja.

Fire isochrone #	BARRA-TA	WN-DAI	WN-GI
1	1.00	1.00	1.00
2	1.00	1.00	1.00
3	1.00	1.00	1.00

Table 35: Median of **Precision**: Comparison of fire simulations using between BARRA-TA and the resampled wind field by WindNinja.

Fire isochrone #	BARRA-TA	WN-DAI	WN-GI
1	0.72	0.75	0.71
2	0.73	0.68	0.70
3	0.75	0.74	0.70

Table 36: Median of **Thread Score**: Comparison of fire simulations using between BARRA-TA and the resampled wind field by WindNinja.

Fire isochrone #	BARRA-TA	WN-DAI	WN-GI
1	0.41	0.42	0.39
2	0.27	0.22	0.27
3	0.28	0.27	0.25

4.2. Comparison with existing fire simulator

There are some existing fire simulators employed in Australia. Their advantages, drawbacks and the solutions provided by Prototype 2, are addressed as seen below.

Table 37: Comparison of fire simulators with advantages and drawbacks

Fire simulator	**Advantages**	**Drawbacks**	**Solution provided by Prototype 1 and 2**
Australis	Fast computation	Distortion of fire direction	Various sampling by 5 geometries in Prototype 2 [1]
Phoenix	Configurable conditions and optimized solutions	- FFDI, which is obsolete, is employed - Weather in rugged terrains are not articulated	- Prototype 2 [1] replaces FFDI with Vesta - Prototypes can ingest topographically sensitive wind with WindNinja - custom-made
Spark	Fast computation, various input formats, user-friendly, versatile, number of fire models for various fuel types	- Weather in rugged terrains are not articulated	- Prototypes can ingest topographically sensitive wind with WindNinja - Prototype 2 [1] provides fuel-to-fire model table - custom made

[1] Prototype 2 is new prototype of fire simulation in this study and upgraded version of Prototype 1 (see external appendix [10]).

The first competitor is Australis, which employs cellular automata mapping events in raster grids. The advantage of cellular automata approach is the speed [19,20]. It can simulate fast because it ingests raster grids, which are binary storage and require less space than vector format. On the other hand, fire tends to move limited direction on cellular automata because a raster grid consists regular shape [21]. Whereas, Prototype 1 and 2 solve this issue by providing various geometries including regular and irregular grids. In addition, a prediction grid can contain more information, such as elapse from the first ignition and status, in Prototype 1 and 2 at the cost of computational performance a vector grid [22].

The second is Phoenix, which is a wildfire risk management model and was developed by Bushfire Cooperative Research Centre (CRC). This tool is a scenario base. Namely, it is possible to input conditions such as venue and datetime of ignitions. Phoenix can simulate fire propagation with likelihood of impacts and propose optimized solutions to mitigate the damage. There are two embedded fire models: CSIRO southern grassland fire spread and McArthur Forest Fire Danger Index (FFDI) version 5 [5,23]. Prototype 2 replaces FFDI with Dry Eucalypt Forest Fire Model (DEFFM or "Vesta"), because FFDI is being obsolete. Phoenix normally provides the 100-200 meters resolution for landscape while the resolution can scale down to 5 meters. Topographical features, such as insolation, are partially considered. However, typical terrain climates, such as valley winds, are not articulated. On the other hand, both Prototype 1 and 2 optionally employ WindNinja, a diagnostic tool, to resample more topographically sensitive wind than the original data reanalyzed by BoM. Phoenix provides risk analyses such as the number of houses being in peril of burning, as integrated software. These estimations can, however, be

decoupled or loosely coupled with fire models from perspective of system architecture so that the functions can be replaced easily [24]. Whereas, both Prototype 1 and 2 can contain statuses and expected elapse from an initial ignition in simulated grid. In addition, these simulation grids can be reused for further statistics such as potentially affected properties separately.

The third is Spark, which is being developed by CSIRO and provides a level set method for various purposes such as research, warning and planning of fire. There are various scales of simulation from laboratory scale to large landscape scale. It allows inputting various formats such as Comma Separated Variable (CSV), image, ESRI vector and raster, NetCDF, geotiff and GDAL. Its computational speed is high because it employs OpenCL, which is application program language (API) enabling concurrent processing. In addition, Spark can be executed in both desktop and cloud-computer. Output data can be visualized on browser using Javascript library, OpenLayers and 2D/3D scene through GIS application [25,26]. In short, Spark is flexible, scalable, fast, user friendly and versatile. On the other hand, it does not explicitly measure fire in rugged terrains because Computational Fluid Dynamics (CFD) is not employed to simulate the fire in short period [25]. Prototypes employ CDF directly neither. However, Prototype 2 optionally ingests wind data resampled by WindNinja, which provides the option, conservation of mass and momentum (CoMM). If the CoMM option is on, WindNinja internally executes OpenFoam to resample wind data for downslope accurately at the cost of computational performance.

References

1. Noble, I.R.; Gill, A.M.; Bary, G.A.V. McArthur's Fire-danger Meters Expressed as Equations. *Australian Journal of Ecology* **1980**, *5*, 201–203.
2. Whiteman, C.D. *Mountain Meteorology: Fundamentals and Applications*; Oxford University Press, 2000; ISBN 0-19-803044-4.
3. Zardi, D.; Whiteman, C.D. Diurnal Mountain Wind Systems. In *Mountain weather research and forecasting*; Springer, 2013; pp. 35–119.
4. Sharples, J.J. An Overview of Mountain Meteorological Effects Relevant to Fire Behaviour and Bushfire Risk. *International Journal of Wildland Fire* **2009**, *18*, 737–754.
5. Bushfire Cooperative Research Centre (CRC) Phoenix - a Fire Charateristic Mapping Model Available online: https://www.bushfirecrc.com/sites/default/files/managed/resource/posterproga-tolhurst.pdf (accessed on 5 December 2020).
6. Forthofer, J.M. Modeling Wind in Complex Terrain for Use in Fire Spread Prediction. **2007**.
7. Canonical Ltd *Ubuntu*;
8. Django Software Foundation Geodjango Available online: https://docs.djangoproject.com/en/2.1/ref/contrib/gis/ (accessed on 31 August 2021).
9. PostGIS Project Steering Project; Project Steering Committee PostGIS Available online: http://postgis.net/ (accessed on 31 August 2021).
10. Ozaki, M. *Prototype 2 - Fire Simulator*; Univesity Of Tasmania, 2021;
11. Sullivan, A.L.; Sharples, J.J.; Matthews, S.; Plucinski, M.P. A Downslope Fire Spread Correction Factor Based on Landscape-Scale Fire Behaviour. *Environmental Modelling and Software* **2014**, *62*, 153–163.
12. The Australasian Fire and Emergency Service Authorities Council (AFAC) Australian Fire Danger Rating System - Research Prototype Available online: https://www.afac.com.au/initiative/afdrs/afdrs-publications-and-reports (accessed on 19 May 2020).
13. Land Information System Tasmania LISTMap Available online: http://maps.thelist.tas.gov.au/listmap/app/list/map (accessed on 18 May 2020).
14. Pyrke, A.; Marsden-Smedley, J. Fire-Attributes Categories, Fire Sensitivity, and Flammability of Tasmanian Vegetation Communities. *Tasforests* **2005**, *16*, 35–46.

15. TOA Systems, Inc GPATS Available online: http://www.gpats.com.au/ (accessed on 15 June 2020).
16. CSIRO AWAP Team Australian Water Availability Project Available online: http://www.csiro.au/awap/ (accessed on 1 July 2020).
17. Su, C.-H.; Eizenberg, N.; Steinle, P.; Jakob, D.; Fox-Hughes, P.; White, C.J.; Rennie, S.; Franklin, C.; Dharssi, I.; Zhu, H. BARRA v1. 0: The Bureau of Meteorology Atmospheric High-Resolution Regional Reanalysis for Australia. *Geoscientific Model Development* **2019**, *12*, 2049–2068.
18. Glen, S. Cohen's Kappa Statistic Available online: https://www.statisticshowto.datasciencecentral.com/cohens-kappa-statistic/ (accessed on 30 March 2020).
19. Trucchia, A.; D'Andrea, M.; Baghino, F.; Fiorucci, P.; Ferraris, L.; Negro, D.; Gollini, A.; Severino, M. PROPAGATOR: An Operational Cellular-Automata Based Wildfire Simulator. *Fire* **2020**, *3*, 26.
20. Faggian, N.; Bridge, C.; Fox-Hughes, P.; Jolly, C.; Jacobs, H.; Ebert, B.; Bally, J. Final Report: An Evaluation of Fire Spread Simulators Used in Australia. *Bureau of Meteorology* **2017**.
21. Johnston, P.; Kelso, J.; Milne, G.J. Efficient Simulation of Wildfire Spread on an Irregular Grid. *International Journal of Wildland Fire* **2008**, *17*, 614–627, doi:Prediction of Fire Spread in Grasslands.
22. Ozaki, M.; Aryal, J.; Fox-Hughes, P. Dynamic Wildfire Navigation System. *ISPRS International Journal of Geo-Information* **2019**, *8*, 194.
23. Tolhurst, K.; Shields, B.; Chong, D. Phoenix: Development and Application of a Bushfire Risk Management Tool. *Australian Journal of Emergency Management, The* **2008**, *23*, 47.
24. McGovern, J.; Tyagi, S.; Stevens, M.E.; Mathew, S. Chapter {2} - Service-Oriented Architecture. In *Java Web Services Architecture*; McGovern, J., Tyagi, S., Stevens, M.E., Mathew, S., Eds.; Morgan Kaufmann: San Francisco, 2003; pp. 35–63 ISBN 978-1-55860-900-6.
25. Miller, C.; Hilton, J.; Sullivan, A.; Prakash, M. SPARK – A Bushfire Spread Prediction Tool. *Environmental software systems: infrastructures, services and applications* **2015**, *448*, 262–271, doi:10.1007/978-3-319-15994-2_26.
26. Spark Available online: https://research.csiro.au/spark/ (accessed on 6 December 2020).

Appendix A

Table 38: TASVEG4 with vegetation communities and fire models where flammability and sensitivity are measured by indicators such as extremely high (E), very high (VH), high (H), medium (M), Low (L) and Nil (N), adapted from [13,14]

veg_group	vegcode_description	Tasveg version	flammability	sensitivity	Fire model
Dry eucalypt forest and woodland	(DAC) Eucalyptus amygdalina coastal forest and woodland	0	H	L	FireDryForest
Dry eucalypt forest and woodland	(DAD) Eucalyptus amygdalina forest and woodland on dolerite	0	H	L	FireDryForest
Dry eucalypt forest and woodland	(DAM) Eucalyptus amygdalina forest on mudstone	3	H	L	FireDryForest

Dry eucalypt forest and woodland	(DAS) Eucalyptus amygdalina forest and woodland on sandstone	0	H	L	FireDryForest
Dry eucalypt forest and woodland	(DCO) Eucalyptus coccifera forest and woodland	0	M	H	FireDryForest
Dry eucalypt forest and woodland	(DCR) Eucalyptus cordata forest	0	M	H	FireDryForest
Dry eucalypt forest and woodland	(DDE) Eucalyptus delegatensis dry forest and woodland	0	H	L	FireDryForest
Dry eucalypt forest and woodland	(DGL) Eucalyptus globulus dry forest and woodland	0	H	L	FireDryForest
Dry eucalypt forest and woodland	(DGW) Eucalyptus gunnii woodland	0	M	H	FireDryForest
Dry eucalypt forest and woodland	(DMO) Eucalyptus morrisbyi forest and woodland	0	H	E	FireDryForest
Dry eucalypt forest and woodland	(DNI) Eucalyptus nitida dry forest and woodland	0	H	L	FireDryForest
Dry eucalypt forest and woodland	(DOB) Eucalyptus obliqua dry forest	3	H	L	FireDryForest
Dry eucalypt forest and woodland	(DOV) Eucalyptus ovata forest and woodland	0	H	L	FireDryForest
Dry eucalypt forest and woodland	(DOW) Eucalyptus ovata heathy woodland	0	H	L	FireDryForest
Dry eucalypt forest and woodland	(DPD) Eucalyptus pauciflora forest and woodland on dolerite	3	M	M	FireDryForest
Dry eucalypt forest and woodland	(DPO) Eucalyptus pauciflora forest and woodland not on dolerite	3	M	M	FireDryForest
Dry eucalypt forest and woodland	(DPU) Eucalyptus pulchella forest and woodland	0	H	L	FireDryForest
Dry eucalypt forest and woodland	(DRI) Eucalyptus risdonii forest and woodland	0	H	L	FireDryForest
Dry eucalypt forest and woodland	(DRO) Eucalyptus rodwayi forest and woodland	0	H	L	FireDryForest
Dry eucalypt forest and woodland	(DTD) Eucalyptus tenuiramis forest and woodland on dolerite	0	H	L	FireDryForest
Dry eucalypt forest and woodland	(DTO) Eucalyptus tenuiramis forest and woodland on sediments	0	H	L	FireDryForest
Dry eucalypt forest and woodland	(DVC) Eucalyptus viminalis - Eucalyptus globulus coastal forest and woodland	0	H	L	FireDryForest
Dry eucalypt forest and woodland	(DVG) Eucalyptus viminalis grassy forest and woodland	0	H	L	FireDryForest

Highland and treeless vegetation	(HCH) Alpine coniferous heathland	0	M	E	FireShrublandBelowWoodland
Highland and treeless vegetation	(HCM) Cushion moorland	0	L	VH	FireShrublandWithoutCanopy
Highland and treeless vegetation	(HHE) Eastern alpine heathland	0	M	VH	FireShrublandWithoutCanopy
Highland and treeless vegetation	(HHW) Western alpine heathland	0	M	VH	FireShrublandWithoutCanopy
Highland and treeless vegetation	(HSE) Eastern alpine sedgeland	0	H	M	FireShrublandWithoutCanopy
Highland and treeless vegetation	(HSW) Western alpine sedgeland/herbland	0	H	M	FireShrublandWithoutCanopy
Modified land	(FAC) Improved pasture with native tree canopy	4	H	L	FireShrublandBelowWoodland
Modified land	(FAG) Agricultural land	0	M	L	FireGrassland
Modified land	(FPE) Permanent easements	0	N	N	
Modified land	(FPF) Pteridium esculentum fernland	0	VH	L	FireGrassland
Modified land	(FPH) Plantations for silviculture - hardwood	0	M	E	FireDryForest
Modified land	(FPS) Plantations for silviculture - softwood	0	M	E	FireDryForest
Modified land	(FPU) Unverified plantations for silviculture	0	M	E	FireDryForest
Modified land	(FRG) Regenerating cleared land	0	M	L	FireGrassland
Modified land	(FUM) Extra-urban miscellaneous	0	N	N	
Modified land	(FUR) Urban areas	0	N	N	
Modified land	(FWU) Weed infestation	0	VH	L	FireGrassland
Moorland, sedgeland and rushland	(MBE) Eastern buttongrass moorland	0	VH	L	FireButtongrass
Moorland, sedgeland and rushland	(MBP) Pure buttongrass moorland	0	VH	L	FireButtongrass
Moorland, sedgeland and rushland	(MBR) Sparse buttongrass moorland on slopes	0	VH	L	FireButtongrass
Moorland, sedgeland and rushland	(MBS) Buttongrass moorland with emergent shrubs	0	VH	L	FireButtongrass
Moorland, sedgeland and rushland	(MBW) Western buttongrass moorland	0	VH	L	FireButtongrass

Moorland, sedgeland and rushland	(MDS) Subalpine Diplarrena latifolia rushland	0	M	M	FireButtongrass
Moorland, sedgeland and rushland	(MGH) Highland grassy sedgeland	0	H	M	FireButtongrass
Moorland, sedgeland and rushland	(MRR) Restionaceae rushland	0	VH	L	FireButtongrass
Moorland, sedgeland and rushland	(MSW) Western lowland sedgeland	0	VH	L	FireButtongrass
Native grassland	(GCL) Lowland grassland complex	0	H	L	FireGrassland
Native grassland	(GHC) Coastal grass and herbfield	0	H	L	FireGrassland
Native grassland	(GPH) Highland Poa grassland	0	H	M	FireGrassland
Native grassland	(GPL) Lowland Poa labillardierei grassland	0	H	L	FireGrassland
Native grassland	(GSL) Lowland grassy sedgeland	3	H	L	FireGrassland
Native grassland	(GTL) Lowland Themeda triandra grassland	0	H	L	FireGrassland
Non eucalypt forest and woodland	(NAD) Acacia dealbata forest	0	M	H	FireDryForest
Non eucalypt forest and woodland	(NAF) Acacia melanoxylon swamp forest	0	M	H	FireWetForest
Non eucalypt forest and woodland	(NAL) Allocasuarina littoralis forest	0	H	L	FireDryForest
Non eucalypt forest and woodland	(NAV) Allocasuarina verticillata forest	0	M	L	FireDryForest
Non eucalypt forest and woodland	(NBA) Bursaria - Acacia woodland	0	H	L	FireDryForest
Non eucalypt forest and woodland	(NLE) Leptospermum forest	0	H	M	FireDryForest
Non eucalypt forest and woodland	(NLM) Leptospermum lanigerum - Melaleuca squarrosa swamp forest	0	M	H	FireDryForest
Non eucalypt forest and woodland	(NLN) Subalpine Leptospermum nitidum woodland	0	M	M	FireDryForest
Other natural environments	(OAQ) Water, sea	0	N	N	
Other natural environments	(ORO) Lichen lithosere	0	N	N	
Other natural environments	(OSM) Sand, mud	0	N	N	
Rainforest and related scrub	(RCO) Coastal rainforest	0	L	VH	FireWetForest
Rainforest and related scrub	(RFE) Rainforest fernland	0	L	H	FireWetForest
Rainforest and related scrub	(RFS) Nothofagus gunnii rainforest scrub	0	L	E	FireWetForest

Rainforest and related scrub	(RHP) Lagarostrobos franklinii rainforest and scrub	0	L	E	FireWetForest
Rainforest and related scrub	(RKF) Athrotaxis selaginoides - Nothofagus gunnii short rainforest	0	L	E	FireWetForest
Rainforest and related scrub	(RKP) Athrotaxis selaginoides rainforest	0	L	E	FireWetForest
Rainforest and related scrub	(RKS) Athrotaxis selaginoides subalpine scrub	0	M	E	FireWetForest
Rainforest and related scrub	(RKX) Highland rainforest scrub with dead Athrotaxis selaginoides	0	L	E	FireWetForest
Rainforest and related scrub	(RML) Nothofagus - Leptospermum short rainforest	0	L	VH	FireWetForest
Rainforest and related scrub	(RMS) Nothofagus - Phyllocladus short rainforest	0	L	VH	FireWetForest
Rainforest and related scrub	(RMT) Nothofagus - Atherosperma rainforest	0	L	VH	FireWetForest
Rainforest and related scrub	(RMU) Nothofagus rainforest (undifferentiated)	3	L	VH	FireWetForest
Rainforest and related scrub	(RPF) Athrotaxis cupressoides - Nothofagus gunnii short rainforest	0	L	E	FireWetForest
Rainforest and related scrub	(RPW) Athrotaxis cupressoides open woodland	0	M	E	FireWetForest
Rainforest and related scrub	(RSH) Highland low rainforest and scrub	0	L	VH	FireWetForest
Saltmarsh and wetland	(AAP) Alkaline pans	0	VH	L	FireGrassland
Saltmarsh and wetland	(AHL) Lacustrine herbland	0	L	L	FireGrassland
Saltmarsh and wetland	(AHS) Saline aquatic herbland	0	L	L	FireGrassland
Saltmarsh and wetland	(ARS) Saline sedgeland / rushland	3	L	L	FireGrassland
Saltmarsh and wetland	(ASF) Fresh water aquatic sedgeland and rushland	0	H	L	FireGrassland
Saltmarsh and wetland	(ASP) Sphagnum peatland	0	L	H	FireButtongrass
Saltmarsh and wetland	(ASS) Succulent saline herbland	0	L	L	FireGrassland
Saltmarsh and wetland	(AUS) Saltmarsh (undifferentiated)	0	L	L	FireGrassland
Saltmarsh and wetland	(AWU) Wetland (undifferentiated)	0	L	L	FireGrassland
Scrub, heathland and coastal complexes	(SAL) Acacia longifolia coastal scrub	0	M	M	FireShrublandBelowWoodland

Scrub, heathland and coastal complexes	(SBM) Banksia marginata wet scrub	0	H	M	FireShrub-landBelow-Woodland
Scrub, heathland and coastal complexes	(SBR) Broad-leaf scrub	0	M	H	FireShrub-landBelow-Woodland
Scrub, heathland and coastal complexes	(SCH) Coastal heathland	0	VH	L	FireShrub-landBelow-Woodland
Scrub, heathland and coastal complexes	(SED) Eastern scrub on dolerite	3	M	L	FireShrub-landBelow-Woodland
Scrub, heathland and coastal complexes	(SHS) Subalpine heathland	0	M	M	FireShrub-landBelow-Woodland
Scrub, heathland and coastal complexes	(SHW) Wet heathland	0	VH	L	FireShrub-landBelow-Woodland
Scrub, heathland and coastal complexes	(SLG) Leptospermum glaucescens heathland and scrub	3	VH	L	FireShrub-landBelow-Woodland
Scrub, heathland and coastal complexes	(SLL) Leptospermum lanigerum scrub	3	H	L	FireShrub-landBelow-Woodland
Scrub, heathland and coastal complexes	(SLS) Leptospermum scoparium heathland and scrub	3	H	L	FireShrub-landBelow-Woodland
Scrub, heathland and coastal complexes	(SMM) Melaleuca squamea heathland	0	H	L	FireShrub-landBelow-Woodland
Scrub, heathland and coastal complexes	(SMR) Melaleuca squarrosa scrub	0	H	M	FireShrub-landBelow-Woodland
Scrub, heathland and coastal complexes	(SRE) Eastern riparian scrub	0	M	H	FireShrub-landBelow-Woodland
Scrub, heathland and coastal complexes	(SRF) Leptospermum with rainforest scrub	0	L	VH	FireShrub-landBelow-Woodland
Scrub, heathland and coastal complexes	(SRH) Rookery halophytic herbland	3	H	VH	FireShrub-landBelow-Woodland
Scrub, heathland and coastal complexes	(SSC) Coastal scrub	0	H	M	FireShrub-landBelow-Woodland
Scrub, heathland and coastal complexes	(SSW) Western subalpine scrub	0	M	M	FireShrub-landBelow-Woodland
Scrub, heathland and coastal complexes	(SWW) Western wet scrub	0	H	M	FireShrub-landBelow-Woodland

Wet eucalypt forest and woodland	(WBR) Eucalyptus brookeriana wet forest	0	M	H	FireWetForest
Wet eucalypt forest and woodland	(WDB) Eucalyptus delegatensis forest with broad-leaf shrubs	0	M	H	FireWetForest
Wet eucalypt forest and woodland	(WDL) Eucalyptus delegatensis forest over Leptospermum	0	M	H	FireWetForest
Wet eucalypt forest and woodland	(WDR) Eucalyptus delegatensis forest over rainforest	0	M	VH	FireWetForest
Wet eucalypt forest and woodland	(WDU) Eucalyptus delegatensis wet forest (undifferentiated)	0	M	H	FireWetForest
Wet eucalypt forest and woodland	(WGL) Eucalyptus globulus wet forest	3	M	H	FireWetForest
Wet eucalypt forest and woodland	(WNL) Eucalyptus nitida forest over Leptospermum	0	M	H	FireWetForest
Wet eucalypt forest and woodland	(WNR) Eucalyptus nitida forest over rainforest	0	M	VH	FireWetForest
Wet eucalypt forest and woodland	(WNU) Eucalyptus nitida wet forest (undifferentiated)	0	M	H	FireWetForest
Wet eucalypt forest and woodland	(WOB) Eucalyptus obliqua forest with broad-leaf shrubs	0	M	H	FireWetForest
Wet eucalypt forest and woodland	(WOL) Eucalyptus obliqua forest over Leptospermum	0	M	H	FireWetForest
Wet eucalypt forest and woodland	(WOR) Eucalyptus obliqua forest over rainforest	0	M	VH	FireWetForest
Wet eucalypt forest and woodland	(WOU) Eucalyptus obliqua wet forest (undifferentiated)	0	M	H	FireWetForest
Wet eucalypt forest and woodland	(WRE) Eucalyptus regnans forest	0	M	H	FireWetForest
Wet eucalypt forest and woodland	(WSU) Eucalyptus subcrenulata forest and woodland	0	M	H	FireWetForest
Wet eucalypt forest and woodland	(WVI) Eucalyptus viminalis wet forest	0	M	H	FireWetForest